Global Environmental Change 72 (2022) 102426

Contents lists available at ScienceDirect

Global Environmental Change

journal homepage: www.elsevier.com/locate/gloenvcha

Exploring river nitrogen and phosphorus loading and export to global coastal waters in the Shared Socio-economic pathways

A.H.W. Beusen [a,b], J.C. Doelman [b], L.P.H. Van Beek [b,c], P.J.T.M. Van Puijenbroek [b], J. M. Mogollón [a,d], H.J.M. Van Grinsven [b], E. Stehfest [b], D.P. Van Vuuren [b,e], A.F. Bouwman [a,b,f,*]

[a] Department of Earth Sciences – Geochemistry, Faculty of Geosciences, Utrecht University, P.O. Box 80021, 3508 TA Utrecht, The Netherlands
[b] PBL Netherlands Environmental Assessment Agency, P.O. Box 30314, 2500 GH The Hague, The Netherlands
[c] Department of Physical Geography, Faculty of Geosciences, Utrecht University, P.O. Box 80.115, 3508 TC Utrecht, The Netherlands
[d] Institute of Environmental Sciences (CML), Leiden University, PO Box 9518, 2300 RA Leiden, The Netherlands
[e] Copernicus Institute of Sustainable Development, Faculty of Geosciences, Utrecht University, P.O. Box 80115, 3508 TC Utrecht, The Netherlands
[f] Frontiers Science Center for Deep Ocean Multispheres and Earth System, and Key Laboratory of Marine Chemistry Theory and Technology, Ministry of Education, Ocean University of China, Qingdao 266100, PR China

ARTICLE INFO

Keywords:
Agriculture
Freshwater
Nitrogen
Phosphorus
Sewage
Scenario

ABSTRACT

This global spatially explicit (0.5 by 0.5 degree) analysis presents the nitrogen (N) and phosphorus (P) inputs, processing and biogeochemical retention and delivery to surface waters and river export to coastal seas according to the five shared socioeconomic pathways (SSP). Four systems are considered: (i) human system; (ii) agriculture; (iii) aquaculture; (iv) nature. Exploring the changes during 1980–2015 and 2015–2050 according to the SSPs shows that the natural nutrient sources have been declining in the past decades and will continue to decline in all SSPs in future decades due to massive land transformations, while agriculture, human sewage and aquaculture are becoming increasingly dominant (globally up to 80% of nutrient delivery). More efforts than those employed in any of the SSPs are needed to slow down the global nutrient cycles. One of the drivers of the proliferation of harmful algal blooms is the tendency towards increasing N:P ratios in global freshwaters and export to the global coastal seas; this is the result of increasing N:P in inputs in food production, more efficient biogeochemical retention of P than of N in river basins, and groundwater N legacies, which seems to be most pronounced in a united world that strives after sustainability. The diverging strategies to achieve UN Sustainable Development Goals 14 (life below water), 2 (zero hunger) and 6 (clean water and sanitation) therefore require a balanced management system for both N and P in all systems, that accounts for future nutrient legacies.

1. Introduction

The global biogeochemical cycles of the plant nutrients nitrogen (N) and phosphorus (P) have been accelerating since pre-industrial times through increasing food and energy production (e.g. Fowler et al., 2013; Smil, 2000). The acceleration of global nutrient cycles has had both positive and negative effects. The increasing use of fertilizers has enabled farmers to produce increasing volumes of food for the rapidly growing human population (Galloway and Cowling, 2002). Since the middle of the 19th century people have been mining deposits of phosphate rock in order to secure P for fertilizer production and industrial uses (Smil, 2000). The Haber-Bosch process for fixing atmospheric N has been employed at an industrial scale to produce N fertilizers since 1913 (Smil, 2001). The major increase of N and P fertilizer production and application began after World War II, simultaneous to the accelerating growth of the global human population.

An unwanted negative effect of increasing fertilizer use is that nutrients have found their way into nearly every inland water body across the globe and are transported in increasing amounts towards coastal waters (Beusen et al., 2016). The increased availability of plant nutrients in aquatic ecosystems has resulted in diverse environmental problems, ranging from groundwater pollution, loss of habitat and biodiversity, hypoxia, proliferation of harmful algal blooms (HAB), and fish kills (Diaz and Rosenberg, 2008; Howarth et al., 2011; Michalak et al., 2013;

* Corresponding author at: Department of Earth Sciences – Geochemistry, Faculty of Geosciences, Utrecht University, P.O. Box 80021, 3508 TA Utrecht, The Netherlands.
E-mail address: lex.bouwman@pbl.nl (A.F. Bouwman).

https://doi.org/10.1016/j.gloenvcha.2021.102426
Received 15 November 2020; Received in revised form 1 November 2021; Accepted 23 November 2021
Available online 8 December 2021

Rabalais et al., 2001; Turner et al., 2003; Vollenweider, 1992). Eutrophication and the associated loss of ecosystem services now rank among the most serious global environmental problems (UN Environment, 2019b).

The aim of this paper is to assess future global changes of nutrient loading in the river continuum from headwaters down to the coastal ocean. This is not an easy task as nutrients in surface water have various natural and anthropogenic sources with completely different economic and societal bases (Seitzinger et al., 2010) and completely different pathways from source to surface water. The world population is projected to grow from current 7.8 (UN, 2020) to 8.5–10 billion inhabitants in 2050 (Riahi et al., 2017). Food production and fertilizer use will have to increase to meet the demand for this growing population; increasing prosperity is expected to lead to shifts in human diets with a growing share of meat and milk (Alexandratos and Bruinsma, 2012; Westhoek et al., 2021), products that are more nutrient intensive than food crops (Galloway et al., 2004; Galloway et al., 1995). This would lead to increasing and spatially concentrated manure production and nutrient pollution. Further, spatial concentration of nutrient losses will increase due to urbanization with more than two-thirds of the world population in 2050 living in cities (Ritchie, 2018). To avoid serious health problems, access to sanitation is required for an additional 2–4 billion inhabitants who need a sewage connection, which will lead to increasing and spatially concentrated nutrient flows if not accompanied by adequate wastewater treatment (Van Puijenbroek et al., 2019). At the same time future agriculture faces finite reserves of rock phosphate for P fertilizer production (Van Vuuren et al., 2010).

Because of the complex behavior and interaction of the global economic and earth systems, future trajectories of global nutrient loading are not well-constrained and may not follow a simple continuation of past trends. Model-based scenario analysis can be used to explore different futures with respect to nutrient loading. The five Shared Socioeconomic Pathways (SSPs) (Riahi et al., 2017) are the most recent set of community scenarios to explore different environmental futures, in particular regarding socio-economic development, agricultural activity, energy system development and water consumption. The SSPs have been implemented with various integrated assessment models including the Integrated Model to Assess the Global Environment (IMAGE) (van Vuuren et al., 2017) (see also https://eartharxiv.org/repository/view/2759/). To accommodate the societal-ecological links relevant to nutrient sources and eutrophication (Mooij et al., 2019) and address the complexity of the biogeochemistry in river landscapes, the Global Nutrient Model (GNM) is used. GNM is part of IMAGE (Stehfest et al., 2014). It uses hydrology as the basis for describing N and P delivery to surface water and in-stream transport and retention processes in streams, rivers, lakes, wetlands and reservoirs with a 0.5 by 0.5 degree resolution (Beusen et al., 2015).

IMAGE-GNM has been used to integrate societal and technological processes and their impact on the change of pools of nutrients in landscapes and impacts on nutrient water quality for the 20th century (Beusen et al., 2016), and will in this paper be used to hindcast the changes in river nutrient sources, delivery and export to the coastal ocean for the period 1980–2015 and to project future changes according to the SSP scenarios for the period 2015–2050. This study is the first global implementation of the SSPs to analyze future global cycles of N and P and consequences for nutrient pollution of surface water. By integrating the various societal drivers of nutrient sources, the results will support policy makers and environmental managers in developing future strategies for mitigation of eutrophication and associated problems in inland and coastal marine waters in the framework of the Sustainable Development Goals (SDG). By linking land-based activities to marine eutrophication, this assessment supports implementation of the UNEP Global Programme of Action (GPA) for the protection of the Marine Environment (United Nations, 1995), links to the recent UNEP resolution on sustainable N management (UNEP, 2019) and the Colombo declaration to halve global N waste by 2030 (UN Environment, 2019a) and ultimately to reconciling the contrasting policy narratives of P scarcity in the food security context and P abundance in the environmental quality context (Smil, 2000). Regarding the consequences for water quality, our results can highlight the integrated impact of the various strategies to achieve the targets of SDG2 (zero hunger), SDG6 (clean water and sanitation) and SDG14 (life below water). The modelled N and P river delivery, retention and export for all rivers in our model in table format discussed in this paper will be available in the Supporting Information. Grid data of all terrestrial N and P budget terms (inputs, crop and grass withdrawal, gaseous emissions, leaching), delivery to surface water from all sources discussed in this paper, retention and export to the coastal ocean is available from https://dataportaal.pbl.nl/downloads/IMAGE/GNM.

2. Material and methods

2.1. Model and data used

Here, a brief overview of the IMAGE-GNM approach is presented. A detailed description can be found elsewhere (Beusen et al., 2015). IMAGE-GNM is coupled to the global hydrological model PCR-GLOBWB (Sutanudjaja et al., 2018; Van Beek et al., 2011) which uses global land cover and climate data for computing the water balance, runoff, discharge and water temperature for each year (Fig. 1). The water and nutrient fluxes through streams and rivers, lakes, wetlands and reservoirs (Fig. 2a) are based on the routing scheme of the PCR-GLOBWB model.

In IMAGE-GNM nutrients are delivered by different sources and pathways within a grid cell (Fig. 2a), and via streams and rivers flowing from upstream grid cells. Two types of nutrient sources are distinguished, i.e. diffuse sources (agriculture, natural ecosystems, aquaculture, weathering, deposition) and point sources (sewage water) (Figs. 1 and 2a).

Point sources of N and P consist of urban and rural wastewater from households and industries that are connected to a sewage system (Figure S1). Household emissions depend on protein intake and P-containing detergent use. The nutrient discharge to surface water is either direct or after treatment. The effluent after treatment depends on the nutrient removal which is based on the relative contribution of four treatment classes (primary, secondary, tertiary and quaternary treatment, each having a typical removal efficiency) which vary from country to country (Van Puijenbroek et al., 2019).

To compute long-term accumulation of nutrients in soils (Bouwman et al., 2017; Zhang et al., 2017) and temporary storage of N and P in groundwater and sediments, IMAGE-GNM calculations cover the full 20th century. As a basis for estimating diffuse nutrient flows from agriculture and natural ecosystems, IMAGE-GNM uses soil nutrient budgets (the difference between inputs and outputs, see Fig. 2b and 2c) which are calculated for every year during the periods 1900–2015 and future years (2015–2050) for each grid cell on the basis of various data sources (see Bouwman et al., 2017) and distributed spatially using the land cover maps that are simulated for each time step.

Spatial land cover distributions for the 1900–1970 period are from the History Database of the Global Environment (HYDE) (Klein Goldewijk et al., 2010) and IMAGE (1970 onwards). The hydrological model PCR-GLOBWB was forced with the reconstructed meteorology for the 20th century using a climate dataset that combines the daily spatial patterns from the ECMWF ERA20C reanalysis (Poli et al., 2016) with monthly observations of the CRU TS 3.2.3 dataset (Harris et al., 2014) spanning the years 1901–2010. For the years 2011–2015, we use the RCP6.0 weather data (see section 2.2.2). Animal populations, excretion rates and manure management systems for 1900 and 1950 were obtained from various sources as described by Bouwman et al. (2013b), and interpolated between 1900 and 1950, and 1950–1970 (the start year of IMAGE simulations). Wastewater flows for 1900–2000 have been described by Morée et al. (2013). For years after 2000 we use data from

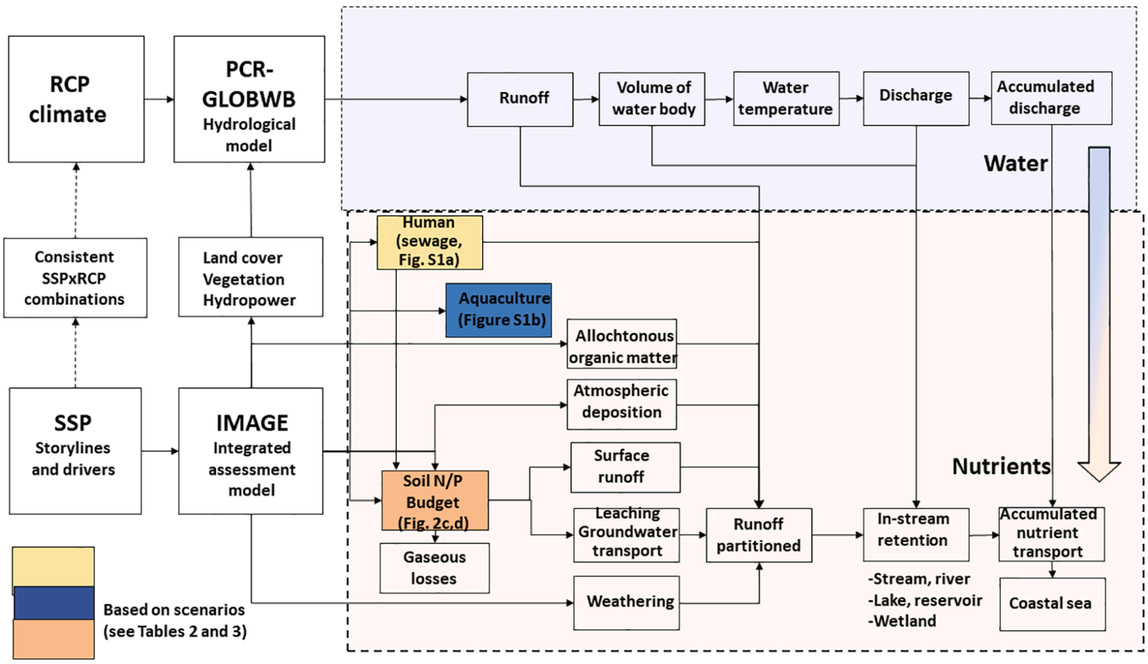

Fig. 1. Scheme of the Integrated Model to Assess the Global Environment (IMAGE) Global Nutrient Model (GNM), including the PCR-GLOBWB model to describe the hydrology. The blue-toned box depicts water fluxes, and the salmon-toned box is the nutrient system. The human (sewage), aquaculture and soil N/P budget boxes indicate where scenario assumptions are used to express the scenario storylines in quantitative terms. (For interpretation of the references to colour in this figure legend, the reader is referred to the web version of this article.)

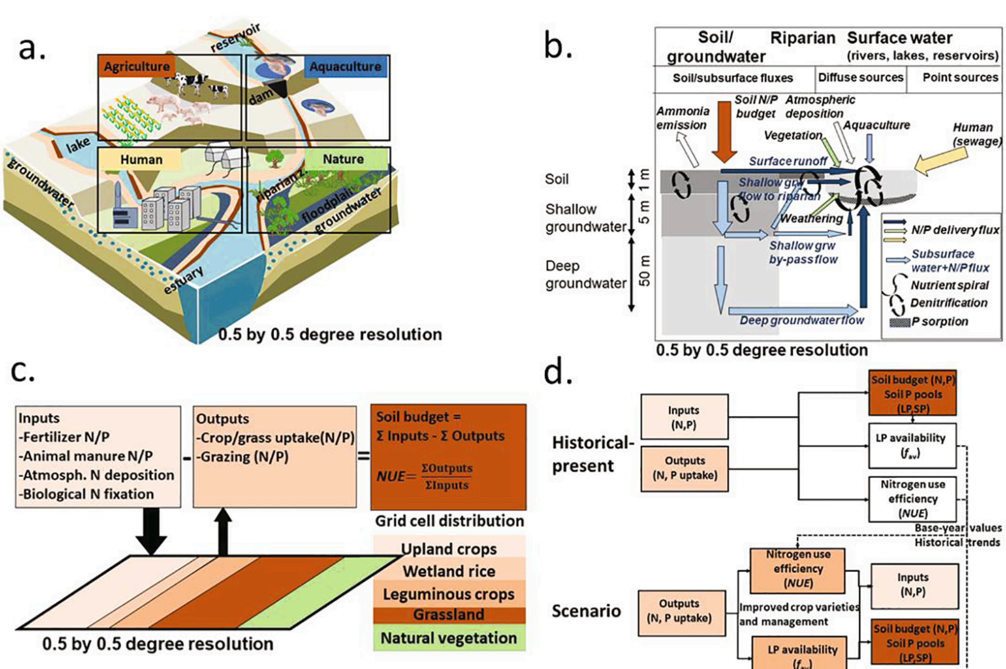

Fig. 2. Schemes of IMAGE-GNM for a) Routing of water (with N and P) in a landscape showing urban areas with sewage outflow, agricultural land, and aquaculture production sites, with floodplains, groundwater, riparian zones, and different water bodies (streams, rivers, lakes, wetlands and reservoirs); each type of water body within a grid cell is defined by an inflow or discharge, depth and area. Floodplains may be temporarily flooded; b) Flows of water and nutrients, retention processes and nutrient delivery by diffuse and point sources of N and P within a grid cell; c) Soil nutrient budget approach with input terms, output terms and budget within each 0.5 by 0.5 degree grid cell; d) Approach for historical years for computing N/P budgets, nitrogen use efficiency (*NUE*) and availability (f_{av}) of P in the labile (*LP*) soil pool, a coefficient that depends on the size of the P pools as a result of historical P budgets. NUE and f_{av} for the base year (2015) and 1980–2015 trends are used as a starting point for the scenarios (see Table 2) to compute required inputs for the output as defined by the SSP considered. Similar schemes for the human/sewage system and aquaculture are shown in Figure S1.

van Puijenbroek et al. (2019). All these data have been prepared and managed within the IMAGE-GNM framework to ensure consistency and avoid discrepancies when coupling time series.

The different components of the land system in IMAGE are simulated for every year in the periods 1970–2015 and future years (2015–2050) by three coupled sub-models (Stehfest et al., 2014), i.e. (i) the agro-economic model MAGNET which determines regional dynamics of food demand, production, trade and intensification based on trends in GDP and population at the level of 26 world regions (Woltjer and Kuiper, 2014), (ii) IMAGE-Land Management which simulates land use dynamics at 5 arc-minutes grid-level for 16 food crop types, 5 animal types, bio-energy, forestry and built-up area (Doelman et al., 2018), and (iii) the LPJmL dynamic global vegetation model which describes potential crop and grass productivity, the carbon and hydrological cycles (both natural and impacted by human use) at 30 arc-minutes resolution (Bondeau et al., 2007). Various upscaling and downscaling functions are used to couple the different resolutions. Data exchange takes place either through hard-coupling with an annual exchange of data or soft-coupling using an iterative approach of scenario data exchange. GNM uses results from IMAGE-Land Management for developments in crop production and cropland that are aggregated to upland crops, N-fixing legumes, wetland rice and grassland with specific fertilizer applications rates (see section 2.2.3). To distribute animal numbers, manure production and grazing land, a distinction is made between mixed and pastoral livestock production systems, and stored manure is distributed over crops and grass as described in Beusen et al. (2008) and Bouwman et al. (2017).

N and P inputs include (where relevant) fertilizer, animal manure, atmospheric deposition and biological N fixation, and outputs are withdrawal by harvesting agricultural crops or grass and forages or by grazing animals. GNM assumes that natural ecosystems are mature and in steady state. This is not correct where soils and vegetation are disturbed or managed, such as re-growth of vegetation after fires, planted forests, or changes in soil and vegetation due to climate warming and CO_2 fertilization. The impact of such disturbances on nutrient loading of rivers is complex and is a topic of future study.

From the N and P budgets (Fig. 2c) and the water flows from the hydrology model (Fig. 1), IMAGE-GNM computes diffuse nutrient transport pathways to groundwater and surface water and air for every year (Figs. 1, 2b). Air emissions of N occur through ammonia volatilization and formation of N_2O and NO_x by denitrification and nitrification (Fig. 1). Ammonia volatilization is based on emission factors presented by Bouwman et al. (2002) that vary with soil, climate, crop and fertilizer properties. Two erosion routes are distinguished, i.e. losses from recent nutrient applications or manure droppings in the form of fertilizer, manure (including direct discharge of manure) or organic matter, and a "memory" effect related to historical changes of the topsoil composition due to long-term soil P application surplus or deficit.

Simulated soil P budgets are often not in balance due to soil accumulation or depletion. Differences between total N inputs and outputs can occur in a number of cases: a) negative budgets in specific grid cells in IMAGE-GNM lead to zero N outputs, since leaching and runoff are computed as a fraction of the surplus; due to aggregation this may lead to a situation with N outputs > inputs at the scale of world regions. b) in dry regions there may be a positive balance (surplus) resulting from deposition and biological N fixation. However, these surpluses are assumed to accumulate in subsurface soil layers such as in Chernozems and other soils in semi-arid zones. In such cases N inputs > outputs; c) in regions with severe soil erosion, this may lead to negative budgets (outputs > inputs).

IMAGE-GNM uses conceptual models for denitrification in soils and groundwater (see text S1). IMAGE-GNM accounts for the memory of groundwater, due to travel times of years to several decades (Fig. 2b). This temporary groundwater storage varies strongly not only due to the geohydrological situation and climate (Van Drecht et al., 2003), but also as a result of the history of fertilizer use and surplus applications (Bouwman et al., 2013a) and leads to legacies of past nutrient management. Further diffuse sources include direct organic matter input to surface water, weathering, aquaculture and atmospheric deposition (Fig. 2a and 2b) (see Text S2).

In-stream retention in all water bodies is calculated using the spiraling approach (Newbold et al., 1981; Stream Solute Workshop, 1990) employed for total N and total P (including all particulate and dissolved N and P forms) (Fig. 2b). Nutrients remaining after retention processes are transported to downstream grid cells and eventually via river mouths to the coastal seas. The spiraling approach uses the depth and the residence time of water in the water body considered, and the net uptake velocity, which is a function of temperature and concentration (for N) and temperature (for P). PCR-GLOBWB lacks description of rivers smaller than Strahler order 6 (Strahler, 1957). Lower order streams are parameterized for each grid cell without lakes or reservoirs following the approach presented by Wollheim et al. (2008).

At any location within a river basin, IMAGE-GNM tracks the different sources of nutrients (i.e. input from upstream grid cells, and delivery to the water bodies within the grid cell. Source attribution can be employed for any point in a river basin, by tracking the history of delivery and retention and including delayed inputs from the groundwater system.

The models for soil denitrification and leaching rates, groundwater denitrification, riparian denitrification and outflow, and instream retention are conceptual models, based on available knowledge of the behavior and functioning of whole the systems considered. Validation of each of these models is difficult due to scale problems, differences in sampling frequency and methods, measurement frequency, depth, location and representativeness. Therefore, validation of measured concentrations in water bodies yields a measure of the model performance for describing processes at the scale of the area drained by the area of the river basin upstream of the monitoring station considered. This was done for a range of stations in a number of rivers (Beusen et al., 2016; Beusen et al., 2015). Compared to Beusen et al. (2015), here we used updates of the input data (e.g. corrections by agricultural data by FAO, a new base year (changed from 2000 to 2015), a new version of IMAGE (3.2) and an update of the PCR-GLOBWB model and its hydrology data. Therefore, we validated the simulated discharge and total N and total P concentrations with observations for a series of rivers, and performed a sensitivity analysis by varying a series of model parameters to determine their impact on model results for the year 2015, and for 2050 for the five SSPs (see Text S3).

2.2. *Scenarios*

2.2.1. *General*

The Shared Socio-economic Pathways (SSPs) represent a widely used set of scenarios describing future development of socio-economic and global environmental change parameters based on internally consistent assumptions (Table 1). One element captured in the SSPs is future food demand and production and associated land use. Important drivers for future food demand are population, economic growth and consequent changes in food preferences. In SSP1, progress is made toward sustainable development, with ongoing efforts to achieve sustainable development goals by improving efficiencies and recycling, reducing food wastes, while reducing resource intensity and fossil fuel dependency. SSP2 is a middle of the road scenario, SSP3 portrays a fragmented world with regions differing widely in socio-economic development. SSP4 represents a strongly unequal world with a small elite and a large, poor and vulnerable group. SSP5 involves traditional development with a focus on economic growth relying strongly on fossil fuels (see O'Neill et al., 2014; Riahi et al., 2017).

The SSPs have been implemented with the IMAGE model (van Vuuren et al., 2017), with land-use trends of the IMAGE SSPs specifically described in Doelman et al. (2018). Here we use an updated version of this implementation (IMAGE version 3.2) (see https://eartharxiv.org/repository/view/2759/), using similar assumptions and resulting in similar projections for domestic production and trade of energy, food, feed and biofuel crops, meat and milk, land use and cover projections, greenhouse gas emissions and climate change (Table 1). Although the base year is 2015, all SSPs have the same trajectories for land use between 2015 and 2020 based on SSP2 and from 2021 onwards the scenarios start to deviate.

2.2.2. *Hydrometeorology*

The socio-economic projections can be combined with different climate scenarios described by the Representative Concentration Pathways (RCPs, see van Vuuren et al. (2014)). The RCPs are labelled according to global average radiative forcing values in the year 2100 (RCP2.6, RCP4.5, RCP6, and RCP8.5 leading to 2.6, 4.5, 6.0, and

Table 1
General description of the five SSP scenarios, and their projections for the year 2050 for population, GDP, greenhouse gas (GHG) emissions, temperature increase relative to 1860, equivalent Representative Concentration Pathway (RCP), meat and total crop production, and area of arable land and permanent crops for IND, BRIC, and rest of the world (ROW)* as implemented by the IMAGE team in a base-year update to 2015/2020 of the original SSPs(van Vuuren et al., 2017) with the IMAGE 3.2 model (Stehfest et al., 2014) (see also the IMAGE wiki https://models.pbl.nl/image/index.php/Welcome_to_IMAGE_3.0_Documentation).

	Region *	1980	2015	SSP1	SSP2	2050SSP3	SSP4	SSP5
Keyword				Sustainability	Middle of the Road	Fragmentation	Inequality	Conventional development
Technological development				Rapid	Medium	Slow	Slow	Rapid
Progress towards development goals				Good	Some	Failure to achieve goals	Highly unequal	Market-driven
Resource intensity				Low	Medium	Little progress	Highly unequal	Conventional (fossil fuel)
Food waste				Reduction by 33%	No change	Increase by 33%	No change	Incresase by 33%
Attitude towards environmental problems				Pro-active	Indifferent	Reactive	Reactive	Reactive
Sewage connection				Strong increase	Current trend	Slow	Slow	Strong increase
Wastewater treatment efficiency				High	Current trend	Medium	Medium	High
Meat consumption				Low	Medium	Unequal	Unequal	High
Agricultural nutrient use efficiency (NUE, see Table 2)				High	No change	Low	Low	High, but also exploding food production
Population (10^6 inhabitants)	World	4458	7382	8744	9349	10,034	9308	8825
	IND	885	1055	1200	1174	1015	1114	1338
	BRIC	1989	3107	3248	3454	3715	3235	3251
	ROW	1585	3221	4297	4721	5304	4959	4236
GDP/capita (US$/yr)	World	5058	7879	22,463	16,701	11,501	16,065	28,603
	IND	20,243	35,310	60,864	56,000	51,769	62,548	70,266
	BRIC	871	3629	21,915	14,631	9200	14,694	27,949
	ROW	1833	2992	12,156	8445	5405	6518	15,945
GHG emissions (Pg C-eq/yr)	Global	9	14.0	16.1	20.3	19.6	15.7	32.2
Global mean temperature increase (°C)**	World	0.4	1.1	2.2	2.3	2.3	2.2	2.6
Meat production (Mton/yr)	World	159	397	516	592	618	559	744
	IND	86	122	108	142	144	136	190
	BRIC	37	169	239	251	256	237	320
	ROW	37	105	170	199	218	186	235
Crop production (Mton dm/yr)	World	2266	4567	6258	6664	6792	6311	7253
	IND	791	1109	1222	1357	1341	1325	1488
	BRIC	783	1859	2343	2389	2442	2309	2550
	ROW	692	1599	2693	2917	3009	2676	3214
Area arable and permanent crops (Mha)	World	1445	1596	1623	1834	1961	1787	1887
	IND	439	383	357	388	387	364	383
	BRIC	458	516	472	510	530	487	518
	ROW	548	697	794	936	1045	936	985

* IND = Industrialized, including Canada, USA, Europe, Japan, Oceania; BRIC = Brazil, Russian Federation, India, China; ROW = rest of the world. Countries included in each region are listed in Table S4.
** Relative to 1860.

8.5 W m^{-2}, respectively). We combine each SSPs with a climate scenario based on projected greenhouse gas emissions as calculated by the IMAGE model that matches these forcing levels (van Vuuren et al., 2017) (Fig. 1). This implies a relatively low forcing level (but not low enough to achieve 2.6 W m^{-2}) in the sustainable development SSP1 scenario and a high forcing level in the fossil-fueled rapid growth SSP5 scenario. This leads to the following combinations: SSP1-RCP4.5, SSP2-RCP6.0, SSP3-RCP6.0, SSP4-RCP6.0 and SSP5-RCP8.5. The PCR-GLOBWB hydrology model was run up till the year 2099 using these RCP simulations (Fig. 1) from the HadCM3 Global Circulation Model (MetOffice, 2020) that were bias-corrected with observed weather data over the historical period 1960–1999 (Hempel et al., 2013). In this analysis, data for the period up till 2050 were used.

2.2.3. *Nutrient cycles*

Future synthetic fertilizer N input was obtained from the difference between total required N and P inputs and the inputs from manure, deposition and biological N fixation, which result from the IMAGE scenario implementations. Scenarios for total N and P requirements were constructed on the basis of the simulated crop and grass production and N and P in harvested parts (Table 2) using specific assumptions on fertilizer use efficiency for N and soil P reserves (see Fig. 1). Scenario SSP1 includes better integration of animal manure in crop production systems which leads to significant productivity increases (Zhang et al., 2020), and SSP1 and SSP5 include substitution of traditional synthetic fertilizers by using recycled N and P from human urine obtained from world inhabitants with a new sewage connection after 2015 (see Table 2).

GNM keeps track of soil P reserves using historical data on P inputs, uptake and runoff to calculate soil P pools and availability up to present day (Zhang et al., 2017). The approach accounts for both soil characteristics relevant to P retention and changing land use, which depends on the scenario considered (Mogollón et al., 2018). Improving technology differs in the SSPs and is mimicked by the proportion of the labile soil P pool that is directly available for uptake by plant roots (f_{av}) (Table 2).

The approach for N requirements used the overall N use efficiencies (NUE, NUE = N yield / total N inputs, using aggregated data for all crops) to construct future scenarios (Table 2 and Table S1). For the middle of the road scenario SSP2, the NUE change between 2015 and 2050 was based on the trends that occurred in NUE between 1980 and 2015, with corrections for future N yield change relative to the historical

Table 2
Construction of scenarios for N and P inputs to cropland and grassland.

	Nitrogen inputs in croplands	Phosphorus inputs in croplands	Nitrogen and phosphorus inputs in grasslands
General approach			
	Future N inputs are based the N use efficiency (NUE, NUE = N removal/ total N input). N yields are calculated from the SSP-specific crop production from Van Vuuren et al. (2017) expressed in N using N contents for each of the 160 crops reported by FAO (Lassaletta et al., 2014). For a given NUE, total inputs can be calculated as N yield / NUE. Fertilizer use is the difference between total N inputs, manure, biological N fixation and deposition. Biological N fixation is from production of leguminous crops according to Salvagiotti et al. (2008). Atmospheric deposition and manure production and attribution to cropland and grassland is from Van Vuuren et al. (2017).	Total P requirements are calculated from the SSP-specific crop production expressed in P using P contents for each of the 160 crops reported by FAO. Starting from the labile and stable pool sizes in the base year, the DPPS model computes the P inputs needed to achieve the P uptake demanded in the specific country and scenario. Each scenario has variations of the fraction available P (f_{av}) within the reactive part of the labile soil P pool reflect the various adaptation challenges of the SSP matrix.	N and P requirements in grasslands are calculated as the N deficit, obtained from a budget approach (N/P inputs equal N/P in production of meat, milk and other products plus N/P excretion) for intensive livestock production systems (see Sattari et al., 2016). Contributions from biological N fixation, atmospheric deposition and animal manure droppings and spreading of manure are accounted for to calculate fertilizer inputs. Pastoral grasslands are excluded assuming that synthetic fertilizer use in extensively managed pastoral areas is negligible.
Scenario-specific assumptions			
SSP1	All manure-N that in 2015 ends outside the agricultural system (manure used as fuel or building material) is assumed to be recycled. Human N from urine of inhabitants with a new sewage connection after 2015 is used to replace traditional synthetic N fertilizers. NUE in 2050 is the 2015 value plus 50% of the difference between the 2015 values and those proposed by Zhang et al. (Zhang et al., 2015). NUE values > 0.70 for 2015 exceed the target values for 2050, are assumed to point to soil N depletion, and consequently NUE values decline and converge with the Zhang et al. values.	All manure-P that in 2015 ends outside the agricultural system (manure used as fuel or building material) is assumed to be recycled. f_{av} increases at the same rate as the increase during 1990–2005. Human P from urine of inhabitants with a new sewage connection after 2015 is used to replace traditional synthetic N fertilizers.	SSP1-SSP5: Scenario outcome depends on the grassland extent, ruminant production and manure management in intensive systems, and no further scenario-specific assumptions are made.
SSP2	NUE in 2050 depends on the NUE in 2015 and the change between 1980 and 2015, which is corrected for the future N yield change relative to the historical yield change. NUE values do not exceed those for SSP1. Where past NUE had a negative trend (Eastern Africa, China, and Korea) the future NUE is assumed to decline by < 5% for the period 2015–2050. For China a constant NUE of 0.38 is assumed after 2015.	f_{av} increases by half the rate assumed in SSP1.	
SSP3	NUE in 2050 is the minimum of the 2015 value and the 2050 value for SSP2.	f_{av} increases by one quarter of the rate assumed in SSP1.	
SSP4	High income regions have NUEs equal to those in SSP1, medium income countries assumed values of SSP2 while low-income regions have SSP3 values	f_{av} for top 5 regions with the highest per capita income is assumed to follow the SSP1 trend, those with < 10% of the average of the top 5 income regions to follow the SSP3 trend, and the rest to follow the SSP2 trend.	
SSP5	NUE is equal to SSP2 for all world regions. Human N from urine of inhabitants with a new sewage connection after 2015 is used to replace traditional synthetic N fertilizers.	f_{av} increases at the same rate as in SSP1. Human N from urine of inhabitants with a new sewage connection after 2015 is used to replace traditional synthetic N fertilizers.	

yield change. In SSP1 it was assumed that 50% of the gap between 2015 values and the NUEs proposed by Zhang et al. (Zhang et al., 2015) is bridged, to reflect that these efficiencies can currently only be achieved in experimental farms (Giller et al., 2004). In the fragmented world of SSP3 the efficiency in agriculture was assumed not to change substantially. NUE developments in SSP4 were based on the income level, using SSP1 values for high-income regions, SSP2 values in middle-income regions and SSP3 values in low-income regions. NUE values in SSP5 equal those of SSP2.

Scenarios for wastewater N and P discharge to surface water were derived from relationships between SSP-specific income and protein consumption, sewerage system connection, nutrient removal by wastewater treatment plants, and detergent use, using historical data aggregated to the scale of the 26 IMAGE world regions (Van Puijenbroek et al., 2019) (Table 3). It was assumed that in SSP1 and SSP5, urine from all households with a sewage connection installed after 2015 will be collected (Table 3). The N yield in urine is 80% of total excretion, and that for P 62% (Van Puijenbroek et al., 2019). The N and P collected thus, is used to replace the traditional synthetic fertilizers (Fig. 1). This has also consequences for the discharge of sewage N and P.

For the scenarios for freshwater aquaculture it was assumed that the global mean per capita production of aquaculture fish is constant, and that a change in total production (global population × per capita production) is employed in all currently aquaculture-fish producing countries. The efficiency of feed and nutrient use depends on the feed conversion ratio (FCR) and the fraction of compound feed in the feed ration for the various shellfish and finfish species (Table 3).

Although current policies were not explicitly included in the SSP storylines, much of the plans are reflected in the assumptions of SSP1, in every sector of society. This results in improved wastewater treatment, recycling of nutrients from wastewater, better integration of animal manure in crop systems, and improved nutrient use efficiency

3. Results

Results for the historical 35-year period 1980–2015 and the future SSP scenarios for the coming 35 years (2015–2050) are presented for the world, IND (industrialized countries), BRIC (Brazil, Russian Federation, India, China) and ROW (rest of the world) (see Table S4). Where relevant, results at the scale of the 26 IMAGE regions are also presented (Figures S3a-h for nutrient inputs, delivery to inland waters, and river export to coastal marine waters, and S4a-h for N and P budgets in agriculture). This section subsequently discusses nutrient inputs in the human, agricultural, aquaculture and natural system (Fig. 2a) (section 3.1), nutrient biogeochemical retention prior to discharge to surface water in each of these systems (3.2), in-stream retention (3.3) and river

Table 3
Construction of scenarios for N and P emission in wastewater from human and industrial wastewater and aquaculture.

A. Wastewater		
General approach		
	Nutrient excretion by humans is computed on the basis of GDP-protein intake relationship, from the actual level for each country, and with a time-variable multiplier for industrial emissions. Assuming that the N content of proteins is 16%, a P:N ratio of 1:10 is used for calculating P emissions. Nutrient discharge is based on relationships between per capita GDP, sewage connection, wastewater treatment and its removal efficiency using aggregated data at the scale of 26 IMAGE world regions. Apart from differences in GDP and population growth between the SSPs, additional assumptions are used for the maximum achievable nutrient removal and sewage connection of rural populations. Details on the model and parameter values can be found in Puijenbroek et al.(2019).	
Scenario-specific assumptions		
SSP1	Maximum nutrient removal of 95%, by introduction of quaternary wastewater treatment; up to 50% of rural population will have sewage connection. Urine from all households with a sewage connection installed after 2015 will be collected used to replace the traditional synthetic fertilizers. The N yield in urine is 80 and that of P is 62% % of total excretion (Van Puijenbroek et al., 2019).	
SSP2	Maximum nutrient removal of 90%, by introduction of quaternary wastewater treatment; up to 30% of rural population will have sewage connection	
SSP3	Maximum nutrient removal of 85% (=current maximum); up to 10% of rural population will have sewage connection	
SSP4	Maximum nutrient removal of 85% (=current maximum); up to 10% of rural population will have sewage connection	
SSP5	Maximum nutrient removal of 95%, by introduction of quaternary wastewater treatment; up to 50% of rural population will have sewage connection. Urine from all households with a sewage connection installed after 2015 will be collected used to replace the traditional synthetic fertilizers. The N yield in urine is 80 and that of P is 62% % of total excretion (Van Puijenbroek et al., 2019).	
B. Aquaculture		
General approach		
	The aquaculture nutrient budget model (i) feed inputs, filtered suspended matter, feed conversion, nutrients in fish and aquatic plants, (ii) outflows in the form of feces and pseudo-feces and dissolved nutrients and (iii) the retention and recycling in pond systems (Bouwman et al., 2013b; Bouwman et al., 2011). Individual species reported by (FAO, 2020) within crustaceans, seaweed, fish and mollusks are aggregated to the International Standard Statistical Classification of Aquatic Animals and Plants (ISSCAAP) groups, for which production characteristics are specified. The major scenario variables employed is the feed conversion ratio (FCR), i.e. the ratio feed input to production, and the fraction compound feed in the fish ration (FRAC_COMP for finfish). FCR is used where relevant, e.g. for shrimp and finfish cultivation, and not for filter-feeding bivalves. Below the FCR changes (negative indicates an efficiency improvement; minimum value for FCR is 1.0) for the period up till 2050 are presented.	
Scenario-specific assumptions		
	Shellfish (FCR)	Finfish (FCR_Comp and Frac_Comp)
SSP1	−40%	Frac_Comp + 20%; FCR_Comp decline is 2x that of 2000–2010
SSP2	−5%	Frac_Comp + 20%; FCR_Comp decline is 2x that of 2000–2010
SSP3	no change	Frac_Comp and FCR_Comp no change
SSP4	−15%	Frac_Comp + 15%; FCR_Comp decline is equal to that of 2000–2010
SSP5	−40%	Frac_Comp + 20%; FCR_Comp decline is 2x that of 2000–2010

nutrient export to the coastal ocean (3.4).

3.1. Nutrient inputs

3.1.1. Historical period

Nutrient inputs have changed dramatically in the past 35 years. The global N (from 308 to 430 Tg yr^{-1}) and P cycles (31 to 45 Tg yr^{-1}) increased by close to 40% between 1980 and 2015 (Fig. 3a). A large part of this increase was due to growing nutrient inputs in agriculture to produce the food for the growing human population, which increased by almost 3 billion inhabitants (Table 1). Food consumption in terms of N and P intake almost doubled (Fig. 3a), which reflects population growth and a shift towards more consumption of meat and dairy along with growing incomes (Table 1). However, nutrient flows related to food consumption are a minor term compared to those in agriculture (Figs. 3 and 4), reflecting the low nutrient efficiencies in current food systems.

While total agricultural N inputs in the industrialized countries in 1980 and 2015 were similar, P inputs even declined, which indicates that the increase in other parts of the world was very large. Agricultural N inputs in industrialized countries declined by 2%, and P inputs by 30% (Fig. 4b), while human N and P intake increased by close to 30% during 1980–2015. Within industrialized countries the pattern is diverse. Some regions showed a rapid decline of N inputs between 1980 and 2015 (Western and Eastern Europe, Japan), some had an increase (Canada) and some only slight changes (USA, Oceania) (Figure S4b-c). For P, there was a decline in USA, Western and Eastern Europe and Japan, an increase in Canada and only slight changes in Oceania (Figure S4b-c).

About 60% of the 122 Tg yr^{-1} increase in the global N input has occurred in the BRIC countries (primarily in agriculture), and another 39% in the ROW countries (Figs. 3 and 4). The BRIC countries contributed an even larger share to the P increase. The human N and P intake also increased strongly in both BRIC and ROW countries. Aquaculture in BRIC countries was responsible for 77% of global N inputs in that sector in 2015, primarily in China and India. Within the BRIC countries these increases in N and P inputs are similar except for the Russian Federation that experienced a major decrease of N and P inputs in agriculture. (Figure S4a) The regions included in ROW show similar increases (Figure S4d-h), except for Ukraine (decline) and Asia-Stan (only slight change) (Figure S4g).

The various inputs in the agricultural nutrient budgets have changed in absolute and relative terms. Global fertilizer N inputs increased by 82%, manure N use by 22%, and input from biological N fixation by 51% (Figure 5 and S5). The relative contribution of global N fertilizer to total N input increased from 29 to 36%. Global food production relied even more heavily on P fertilizer (increase from 48 to 53%) (Figure 6 and S6). The picture for the three world regions is completely different, whereby ROW relied much more on animal manure (47% in 1980, 42% in 2015) and N fixation (19–18%) for N supply, and animal manure (66% over the 1980–2015 period) for P supply, with a modest role for fertilizer P (33%). Synthetic fertilizer use in some regions within ROW is small compared to other inputs (Western and Eastern Africa, and rest Southern Africa, Figure S4e-f). In the industrialized countries, P fertilizer use decreased due to a combination of factors, e.g. environmental policy and improved nutrient management. As a result, there was a decline of the share of P fertilizer to the (declining) total P inputs (11.7 to 8.2 Tg P yr^{-1}) from 58% (6.8 Tg P yr^{-1}) to 53% (4.3 Tg yr^{-1}) between 1980 and 2015, while the share of animal manure increased from 41% to 47%. In contrast, the proportion of N fertilizer, manure N and N fixation in total N supply was rather stable in industrialized countries. Despite declining fertilizer use after the fall of the Soviet Union (Figure S4a) (van Dijk et al., 2016), BRIC as a whole showed a rapid increase of N (156%) and P fertilizer (221%) between 1980 and 2015, and the share of fertilizers to total inputs grew from 34% to 45% for N and from 47% to 66% for P.

3.1.2. Future scenarios

Changes in the coming 35 years will also be large with a further intensification of both the N and P cycles in all SSPs (Figs. 3 and 4). At the global scale this increase is most pronounced in SSP3 (36% for N and 53% for P) (due to fast growth of population and demand for crops and animal products, see Table 1) while in the sustainability scenario SSP1 (lowest population and food production of all SSPs) this increase is modest (6% for N and 11% for P). In the industrialized countries, the total N inputs will grow by 19–28% in SSP2, SSP3 and SSP5, stabilization in SSP4 and decline in SSP1. Total N and P inputs in BRIC countries stabilize in SSP1 and increase by 25–28% in SSP3 and less so in other

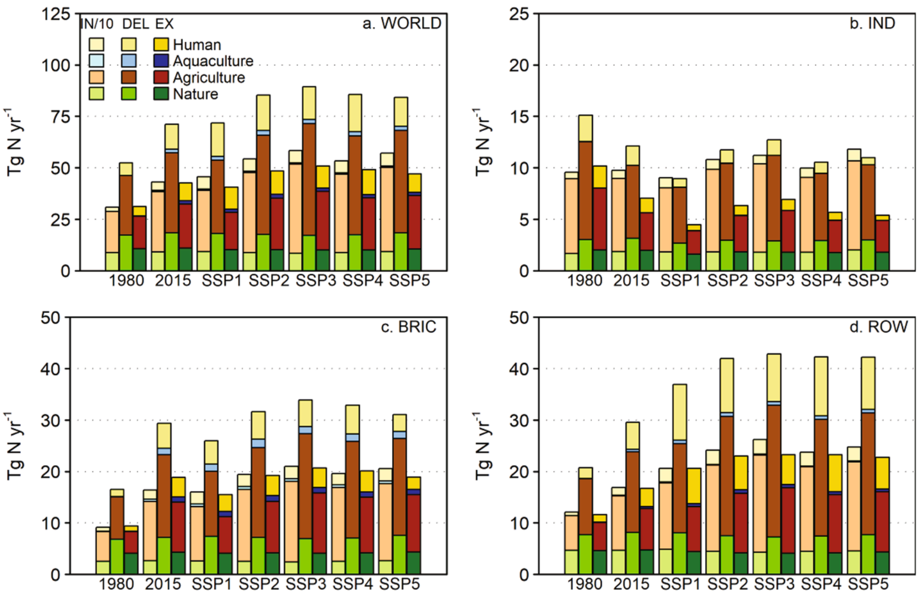

Fig. 3. Nitrogen Inputs (IN), Delivery (DEL) to surface water, and river Export (EX) to the coastal ocean for the human, agriculture, aquaculture and natural systems for the world, IND, BRIC and ROW countries for 1980, 2015 and 2050 for the five SSPs. Countries included in these regions are listed in Table S4. The inputs include: human system - nitrogen consumption; agriculture system - nitrogen fertilizer, animal manure, biological nitrogen fixation and atmospheric deposition; aquaculture system – feed nitrogen; natural system – biological nitrogen fixation, atmospheric deposition. Delivery is the direct discharge to surface water from aquaculture and the from sewage in the human system, for agriculture and natural systems nutrients are delivered through groundwater discharge and surface runoff, and for natural systems including atmospheric nitrogen deposition onto surface water and nitrogen in litter from vegetation in flooded areas.

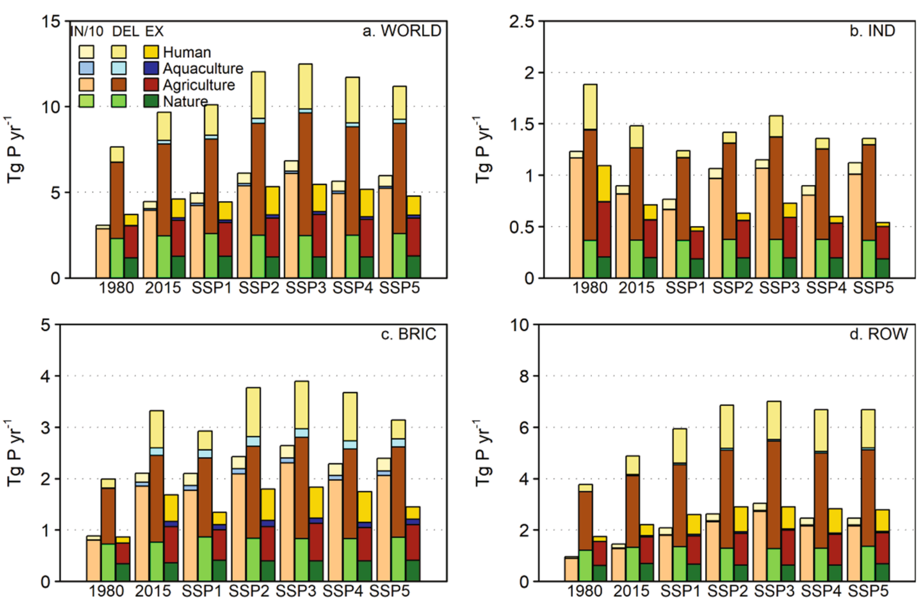

Fig. 4. Phosphorus inputs (IN), delivery (DEL) to surface water, and river export (EX) to the coastal ocean for the human, agriculture, aquaculture and natural systems for the world, IND, BRIC and ROW countries for 1980, 2015 and 2050 for the five SSPs. Countries included in these regions are listed in Table S4. The inputs include: human system - phosphorus consumption; agricultural system - phosphorus fertilizer and animal manure; aquaculture system – feed phosphorus; natural system – none. Delivery in the direct discharge to surface water from aquaculture and the from sewage in the human system, for agriculture and natural systems phosphorus is delivered via surface runoff, and for natural systems via weathering and phosphorus in litter from vegetation in flooded areas.

SSPs, while most of the global growth of N and P inputs is expected to occur in ROW countries. This is primarily the result of the growing demand for food and animal products in the developing economies (Table 1) which induces a massive growth in fertilizer use, in the sustainability scenario SSP1 by 36% for N and 116% for P (Figs. 5 and 6). The growth of total N and P inputs in the other scenarios is much larger than in SSP1 (Figs. 3 and 4). The rapid growth of food production in ROW is also reflected by the growth of human N and P consumption in the coming 35 years by 85% in SSP3 and 72% in SSP1. Feed inputs for aquaculture are projected to increase further in the BRIC countries, in SSP2 by>25% (Figs. 3 and 4).

The assumptions on the development of NUE (Table S1) have a major impact on the projected N fertilizer use, which in 2050 is close to 168 Tg N yr^{-1} (+55%) for SSP3 and SSP5, and shows a modest increase of 14% in SSP1 (Figure 5 and S5). However, in SSP1 about 24 Tg N yr^{-1} of N and 1 Tg yr^{-1} of P fertilizer stems from human urine collected from households with a new sewage connection. In SSP5 the contribution of human urine is even higher (26 Tg yr^{-1}N and 2 Tg P yr^{-1}, respectively, in 2050) (Figures 5, S5 and 6 and S6). According to the middle of the road assumptions for SSP2, N fertilizer use will increase by 47% between 2015 and 2050, which is a continuation of the 82% increase in the previous 35 year period. While N fertilizer use will increase by 16% in industrialized countries according to SSP2, there is an increase by 30% in BRIC countries, and by 117% in ROW countries. Within BRIC, all subregions show increasing N fertilizer use except China with a stabilization (Figure S4a). Within ROW, nearly all regions will increase N fertilizer use in SSP2 (Figure S4d-h). Global P fertilizer use is projected to increase by 47% in SSP2, with a large part of the ~10 Tg P yr^{-1} increase occurring in ROW (Fig. 6) which is projected in nearly all ROW subregions (Figure S4d-h).

3.2. Nutrient retention prior to discharge to surface water

The difference between the total inputs and the delivery to surface water (Figs. 3 and 4) is the biogeochemical retention in landscapes and in wastewater treatment (Figure S2). In landscapes the soil–plant

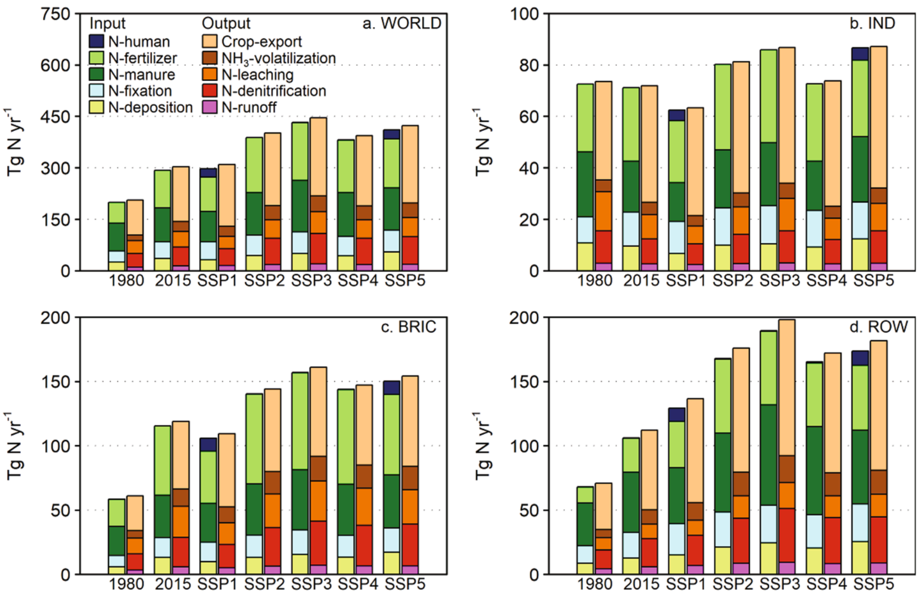

Fig. 5. N input and outputs in the agricultural system including cropland and grassland for the WORLD, IND, BRIC and ROW countries for 1980, 2015 and 2050 for the five SSPs. Countries included in these regions are listed in Table S4. In SSP1 and SSP5, part of the synthetic fertilizer is replaced by N and P in human urine (80% of total N excretion) collected from all households that are connected to a sewage system after 2015. The same data is presented in kg N per hectare of total agricultural land in Figure S5.

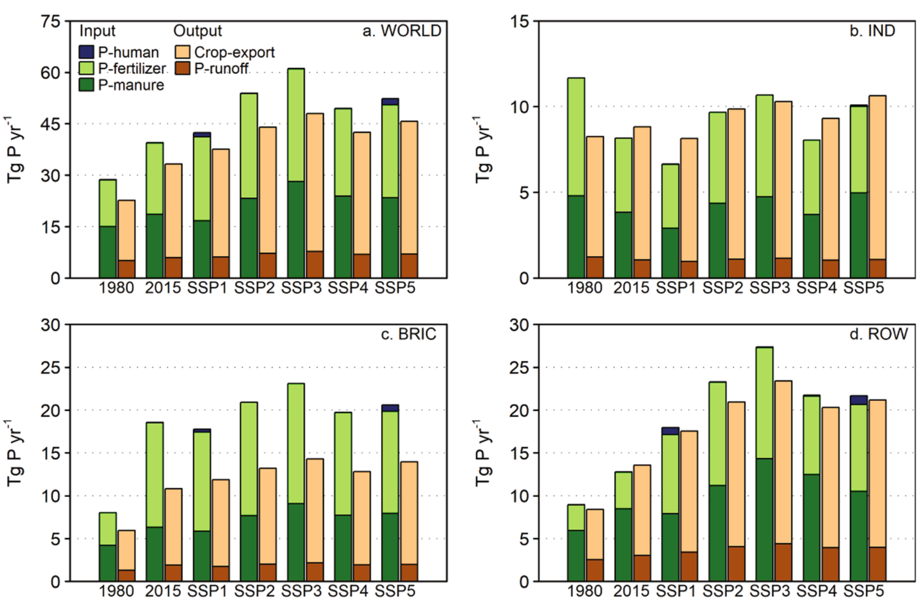

Fig. 6. P input and outputs in the agricultural system including cropland and grassland for the WORLD, IND, BRIC and ROW countries for 1980, 2015 and 2050 for the five SSPs. Countries included in these regions are listed in Table S4. In SSP1 and SSP5, part of the synthetic fertilizer is replaced by N and P in human urine (62% of total P excretion) collected from all households that are connected to a sewage system after 2015. The same data is presented in kg P per hectare of total agricultural land in Figure S6.

retention (section 3.2.1) is represented by uptake by plants and biogeochemical processing in soils. After this first landscape retention, water with dissolved nutrients percolates through the soil and moves through groundwater and riparian zones (section 3.2.2). During this transport there is further biogeochemical retention before the water and nutrients are discharged to surface water bodies. Man-made retention is the nutrient removal from wastewater discharge in treatment plants, and recycling of nutrients in agricultural systems (section 3.2.3).

3.2.1. *Soil-plant retention*

The crop N retention represented by the fraction of N that ends in harvested products (nitrogen use efficiency, NUE) increased slightly from 51 to 55% during 1980–2015, and will increase further to 60% in SSP1 compared to 52% in SSP3 (Fig. 5). The complement of the NUE for global N inputs is either lost to the environment by ammonia loss (8–10%), runoff (4–5%), leaching (15–18%), or removed by denitrification (12–19%). These fractions vary between regions, with NUE values for the SSP1 scenario of up to 67% in industrialized countries, 62% in ROW and 54% in BRIC countries. This implies that the losses to the environment also vary. The N losses to the soil-hydrological system (leaching and runoff) together are globally 17–19%, depending on the scenario, and are highest in BRIC countries (Fig. 5).

The global P use efficiency (PUE) increased from 61% to 69% between 1980 and 2015, while residual P accumulation (21 to 16%) and P runoff (18 to 15%) declined. This is completely different in the various world regions. In the industrialized countries there has been massive P accumulation in soils (Fig. 6) in the 1970 s to 1990 s, which changed in recent years to negative P budgets due to declining P fertilizer use and continued increase of P uptake in Western and Eastern Europe and USA. In the ROW countries the negative soil P budget (inputs < outputs) reflects soil mining with low crop yields at minimal or even absent P inputs, which is apparent in most of the ROW subregions (Figure S4e-j). Similar to the industrialized countries in the 1970 s and 1980 s there is currently P accumulation in soils in BRIC (Fig. 6) which is seen in all subregions except for the Russian Federation (Figure S4a).

Future PUEs diverge, with continued depletion in industrialized countries where farmers benefit from the soil P reserves built up in previous decades. However, in ROW countries there will be soil P mining (see Fig. 6d), and the future increase of nutrients in food production, given the land use projections in each scenario (Table 1), will only be possible with larger inputs of both N and P. Depending on the scenario, there is more or less P accumulation to support future food production (Fig. 6). In BRIC countries, P accumulation is projected to decline from 42% of P inputs in 2015 to 32% in SSP5, which implies that beyond 2050 less P fertilizer is needed to support the same production level.

3.2.2. Groundwater and riparian retention

At the global scale, 29% of the 53 Tg N yr^{-1} that leached from natural and agricultural soils in 1980 was denitrified in groundwater (12 Tg N yr^{-1}) and riparian zones (4 Tg N yr^{-1}). In 2015 this removal increased to 33%, particularly in groundwater. N leaching from soils varies considerably between the SSPs, with a decline by 17% in SSP1 and a 27% increase in SSP3 between 2015 and 2050. Denitrification in groundwater and riparian zones will, as a result, both decline in SSP1 and increase by 29% in SSP3.

3.2.3. Wastewater treatment

Human excreta can be recycled in agriculture, deposited in pit latrines or septic tanks, or discharged via sewage systems with or without treatment. Our approach accounts for the N and P emissions from households with a sewage connection (globally around 40% of the total population, Table 4), the removal in wastewater treatment plants and the effluent to surface water (Table 4). Our results show that at present the overall nutrient removal efficiency is 26% of the emissions from connected households (or circa 10% for emissions from the total population). In the period up till 2050, this removal efficiency is projected to increase to 55% globally, with an increase to > 80% in industrialized countries, up to 60% in BRIC countries, and close to 40% in ROW countries. The nutrient emissions from the 70% of the population lacking a sewage connection offer possibilities for recycling to agriculture and other uses. At present, this is only a very small amount, but for 2050 human waste can play a more prominent role, especially in ROW and BRIC countries (Figs. 5 and 6).

3.3. In-stream retention

Total N delivery is computed for every year and all scenarios as shown for 1980, 2015 and 2050. SSP1 and SSP3 show the largest deviation in 2050 (Fig. 7), and both scenarios indicate a large concentration of nutrient loading in regions with intensive agriculture and high population densities (Fig. 7). The difference between the nutrients delivered to surface water (Fig. 7) and the river export to the coastal ocean (Figs. 3 and 4) is caused by the in-stream retention (Figure S2). Global in-stream N (40–41%) and P retention (54–55%) is stable and not expected to change drastically in the future scenarios. Overall N retention in rivers in IND countries is close the global retention fraction, while that in ROW countries is lower (37–38%).

3.4. Nutrient export

Current global river export amounts to 43 Tg yr^{-1} of N and 5 Tg yr^{-1} of P (Fig. 8 and Figure S7). Global river N export is expected to decline by 5% in SSP1 and to increase in all other scenarios, most rapidly in SSP3 (close to + 20%). Natural sources of N and P show no significant change, but SSP1 shows a decrease of agricultural N (-15%) and P (-7%), while there are major increases in river export from agricultural sources in all other scenarios (+33% for N and + 18% for P in SSP3). N originating from sewage declines in SSP1 and increases in all other SSPs, while P from sewage increases in all scenarios (up to + 49% for P in SSP2). No major changes are projected for the Arctic ocean, while in the Atlantic and Pacific Oceans there is a difference between SSP1 (no major change), and the other scenarios where sewage and agriculture have increasing trends. The most important increase of river nutrient export is projected for the Indian Ocean, where agricultural sources (highest + 60% for N and + 29% for P in SSP3) and sewage (highest + 203% for P in SSP2, >155% for N in SSP1 and SSP4) show large increases.

Table 4
Population with sewage connection, human N emission from connected households, nutrient removal, N effluent, human P emission from connected households, and P effluent for 1980, 2015, and 2050 for the five SSPs for BRIC, IND, ROW countries and the world.

Year/scenario	Aggregated world region BRIC	IND	ROW	World
	Population with sewage connection (% of total population)			
1980	10	64	16	23
2015	38	83	28	40
2050-SSP1	76	95	63	72
2050-SSP2	62	89	50	59
2050-SSP3	46	83	37	45
2050-SSP4	64	91	41	55
2050-SSP5	77	94	66	75
	Human N emission from households with sewage connection (Tg N yr^{-1})			
1980	1.0	3.1	1.3	5.4
2015	4.1	4.0	3.2	11.3
2050-SSP1	13.2	5.8	13.1	32.1
2050-SSP2	11.0	5.3	10.9	27.3
2050-SSP3	8.5	4.2	8.6	21.3
2050-SSP4	10.9	5.2	9.5	25.6
2050-SSP5	13.8	6.5	14.0	34.4
	Nutrient removal in wastewater treatment installations (%)			
1980	3	24	2	15
2015	8	55	15	26
2050-SSP1	57	86	38	55
2050-SSP2	43	77	32	45
2050-SSP3	33	70	26	37
2050-SSP4	44	81	31	46
2050-SSP5	69	90	44	63
	N effluent (Tg N yr^{-1})			
1980	1.0	2.4	1.3	4.6
2015	3.8	1.8	2.7	8.3
2050-SSP1	5.7	0.8	8.1	14.6
2050-SSP2	6.3	1.2	7.5	15.0
2050-SSP3	5.7	1.3	6.4	13.4
2050-SSP4	6.1	1.0	6.6	13.7
2050-SSP5	4.3	0.7	7.8	12.8
	Human P emission from connected households (Tg P yr^{-1})			
1980	0.1	0.6	0.2	0.9
2015	0.9	0.6	0.6	2.1
2050-SSP1	1.4	0.6	1.9	3.8
2050-SSP2	2.5	0.6	2.0	5.0
2050-SSP3	1.9	0.9	1.7	4.4
2050-SSP4	2.3	0.7	1.7	4.8
2050-SSP5	2.1	0.7	2.2	5.0
	P effluent (Tg P yr^{-1})			
1980	0.1	0.4	0.2	0.8
2015	0.7	0.2	0.5	1.4
2050-SSP1	0.5	0.1	1.1	1.6
2050-SSP2	1.2	0.1	1.3	2.5
2050-SSP3	1.1	0.2	1.1	2.4
2050-SSP4	1.1	0.1	1.1	2.2
2050-SSP5	0.6	0.1	1.2	1.8

4. Discussion

4.1. Validation and sensitivity analysis

We validated the uncalibrated IMAGE-GNM in different ways. First, we analyzed if the model can reproduce changing N and P concentrations over long time periods. Secondly, we compared the performance of the model for rivers in tropical and temperate climates. Data for validation are scarce. IMAGE-GNM results for individual rivers are less reliable for small rivers than for large rivers, because of the uncertainty in the spatial patterns of streams and rivers, lakes, reservoirs, precipitation, land use, urban areas, aquaculture, etc. Employing an absolute

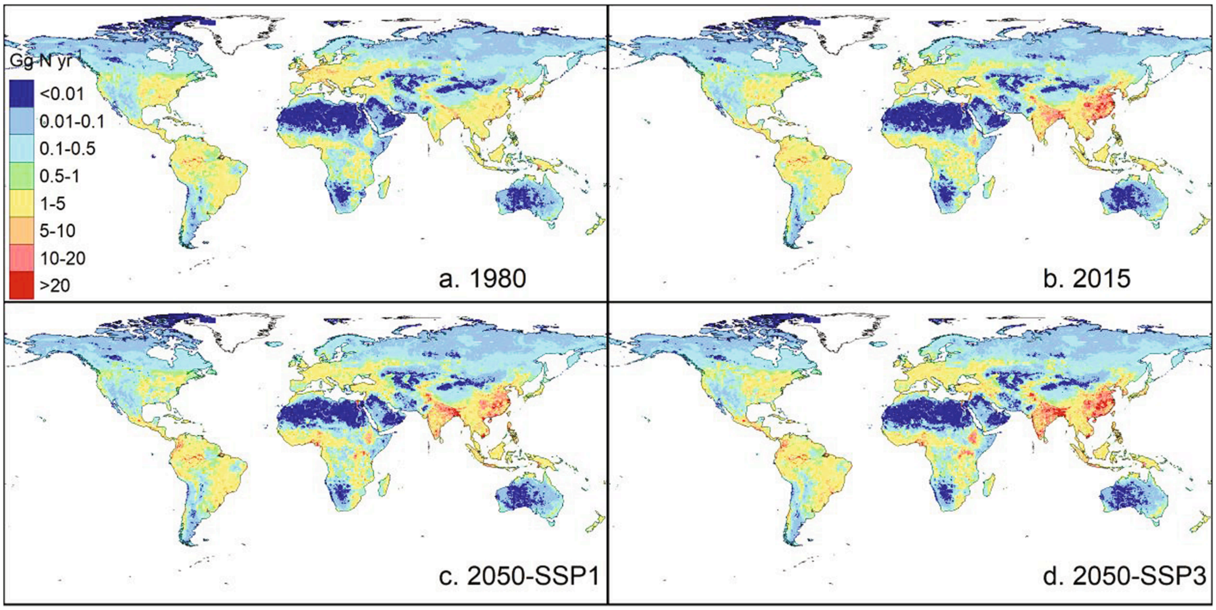

Fig. 7. Maps of N delivery to surface water for 1980 (top left), 2015 (top right) and 2050 for the SSP1 sustainability (bottom left) and SSP2 middle of the road scenario (bottom right).

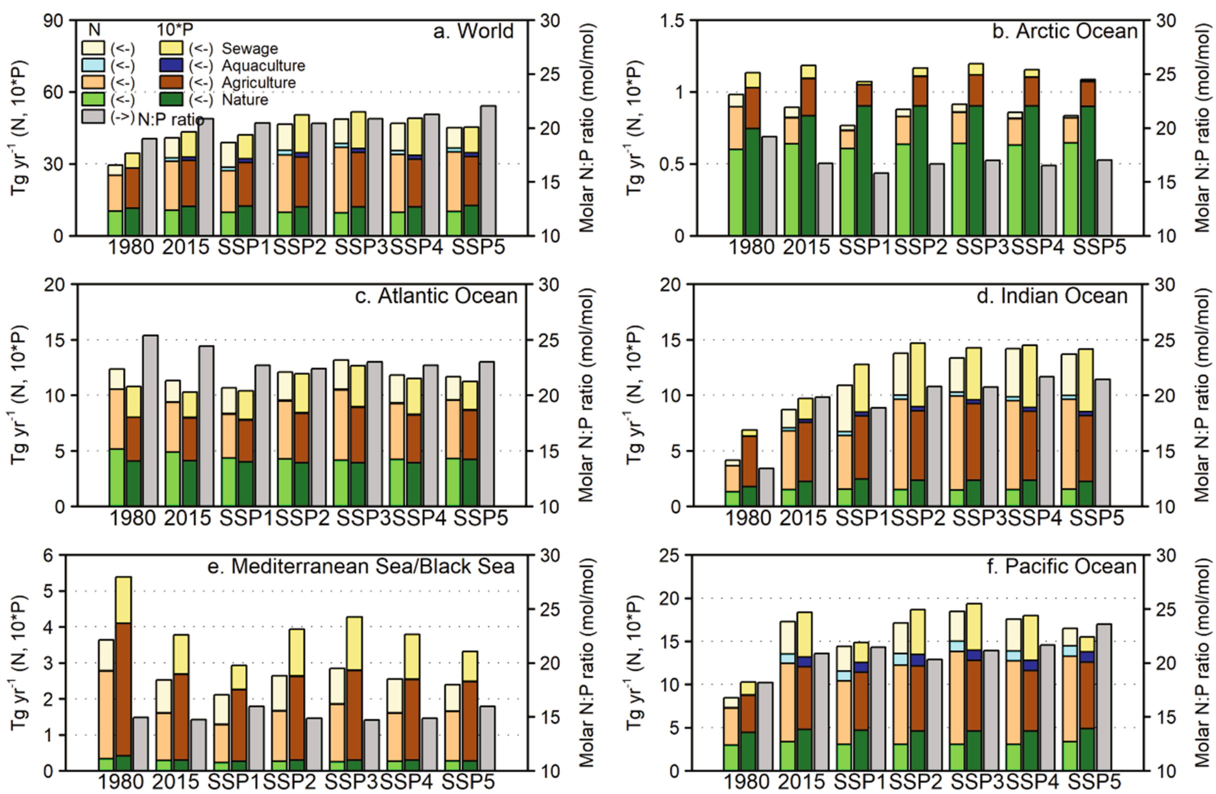

Fig. 8. Annual N and P export and molar N:P ratio for a) all oceans, globally; b) Arctic Ocean; c) Atlantic Ocean; d) Indian Ocean; e) Mediterranean Sea and Black Sea; and f) Pacific Ocean for 1980, 2015 and 2050 for the five SSPs.

minimum of 4 grid cells (10,000 km^2) implies that stations with data for TN and TP are scant. In addition, in the majority of cases TN and TP are not reported, since often organic or particulate forms of N and P not available. Finally, there are only few large rivers where long-term monitoring data are available. Often data represent only 1 year, or even part of a year. Time series are important, because a model used for scenario analysis must be able to show an acceptable agreement over historical time periods of sufficient length with changing conditions (climate, hydrology, land use, urbanization, etc.) so that future projections can be made with confidence.

We use data covering up to 40 years (~1970–2010/2014) for stations closest to the river mouth lacking tidal influence four rivers, i.e. the Meuse and Rhine (Western Europe), Mississippi (USA) and Yangtze (China), to allow for comparing the performance of the model with updated hydrological input. The simulated long-term discharge was within an acceptable Root Mean Square Error (RMSE, see Text S3) of

50% (Beusen et al., 2015) for all rivers (Meuse at Eysden station, Netherlands, 42%; Rhine at Lobith station, Netherlands, 17%; Mississippi at station closest to river mouth with freshwater near St. Francisville, 38%; Yangtze at Datong station, 8%). Validation of the model against time series of total N and total P concentrations showed good agreement for Meuse (RMSE 25% for N and 46% for P concentrations 1970–2010), Rhine (RMSE 33% for N and 38% for P for concentrations 1970–2010) (Figure S10), Mississippi (various stations in Mississippi, Ohio, Arkansas and Missouri rivers, see Table S3; RMSE for 18% for N and 58% for P concentrations 1974–2020) (Figure S11) and Yangtze (RMSE 46% for N and 323% for P concentration) (Figure S12). IMAGE-GNM does reproduce the increasing N and P concentrations in the Yangtze, the declining trend in Rhine (N and P) and Meuse (P), the lack of a trend for N and P concentrations in the Mississippi and of N concentrations in the Meuse. Overall, the updated hydrology did not affect the performance of the model for the Rhine, Meuse and Mississippi.

Secondly, we compared simulated concentrations for 9 tropical (Figure S13a) and 30 temperate rivers (Figure S13b) with reported values that represent the situation in the late 1980 s to early 1990 s except for the Mekong (1980–2015). The agreement for temperate rivers was slightly better ($r = 0.88$; Figure S13) than for the tropical ones ($r = 0.73$).

Figure S13 includes data for three large tropical rivers, i.e. the world's largest river Amazon in South America dominated by natural ecosystems and with low population density, the Mekong river that crosses six Asian countries is densely populated with intensive human agricultural land use and aquaculture, and strong moderation of the hydrology by dams and reservoirs, and the Pearl river (China) with very high population density and agricultural activity, and with limited moderation by dams. Results for the Amazon, are in good agreement with values reported by Forsberg et al (1988) (simulation 0.5 mg N l^{-1} versus reported 0.4 mg N l^{-1}; simulation 0.04 mg P l^{-1} versus reported 0.06 mg P l^{-1} for 1982–1984). TN and TP concentrations for the Mekong for the period 1985–2010 do not show a real trend. IMAGE-GNM overestimates the values reported by Li and Bush (2015) (simulated 0.8 versus observed 0.5 mg N l^{-1}; 0.07 versus 0.05 mg P l^{-1}). The simulated average TN concentration of 1.7 mg N l^{-1} for 1980–1989 for the Pearl exceeds the reported 1.4 mg N l^{-1} for this period by < 20% (RMSE = 30%).

These comparisons of our model for long time series for selected rivers, and data covering shorter periods for other sets of rivers from temperate and tropical climates, differing in size and geological setting, show that IMAGE–GNM shows a fair to good agreement with observations without any tuning of the overall, integrated model. The model reproduces trends over time periods of 30–40 years and does not show systematic over- or underestimation. Therefore, we are confident that IMAGE-GNM can simulate fluxes and trends at the scale of continents or world regions with reasonable accuracy.

Results of the sensitivity analysis of the IMAGE-GNM model for the year 2015 (Tables S2b-c) are similar to the findings reported previously (Beusen et al., 2016; Beusen et al., 2015). Total runoff is an important factor for N and P delivery, retention and river export in 2015 and for the five SSPs. Runoff determines all transport pathways and flows of N (surface runoff, leaching, groundwater flow, and in-stream retention), and it determines the major transport pathway for P, which is surface runoff. Temperature also influences all processes in soils and the hydrosphere, and is important for N delivery, retention and export. In the spiraling method, uptake velocity and all parameters used to calculate the in-stream retention (i.e. L_1, R_1 and v_f) at the sub-grid level are important for total in-stream retention and/or river export. Soil N budgets, wastewater are important for N delivery to surface water and export to coastal waters. For P, the factors that determine the P content of the soil (soil P content and bulk density) are important factors for delivery, implying that residual P accumulation is an important determinant of water quality. The uptake velocity for P is important for both retention and export.

We also analyzed the model sensitivity for the year 2050 for the five SSPs (Tables S2b-c). The model sensitivity of delivery load to surface water and river export for the years 2050 largely differs between scenarios for the N budget in cropland which is largest in SSP3 and SSP5 (lowest efficiencies) and the point source load, which is highest in SSP1 where sewage becomes more important due to high efficiency and large reductions of emissions in agriculture. For P, the uptake velocity is important for in-stream retention and export with small differences between the scenarios, while the importance of P discharge from point sources is important for the delivery load to surface water and export for SSP2 and SSP4.

In the context of the future outlooks in this paper, the sensitivity of model results to changes in scenario assumptions (Fig. 1) is of interest. Here the importance of NUE (Table S1) for the delivery and river export of N was analyzed, together with the nutrient delivery from sewage and aquaculture. Results of this analysis show that fertilizer N use is sensitive to NUE, at the global scale causing a range of −18 to + 38% around the 2050 value of 160 Tg N yr^{-1} (Table S2). The resulting relative variation for total N fertilizer use based on NUE variation is somewhat larger for IND and BRIC than for ROW countries, reflecting the share of fertilizers in total N inputs. The impact of the variation of NUE, sewage and aquaculture on global river export is −12% to + 40% (Table S2), and the largest impact of these assumptions is seen in IND countries.

Climate does influence the whole system, from leaching, groundwater transport, travel times and in-stream retention. The factors temperature, N concentration and runoff turn out to be important for N, and runoff is the most important factor for P, but the small differences between SRC values for these factors reflect the small difference between the climate scenarios in 2050, which start to really diverge after 2050.

4.2. Results in perspective

The agricultural N and P budgets calculated for past decades have been extensively discussed in recent work (Bouwman et al., 2017). Here the estimated future agricultural nutrient inputs are compared with projections by FAO and results from an earlier scenario study. The global fertilizer use projections for 2050 for the middle of the road SSP2 scenario (160 Tg N yr^{-1} and 31 Tg P yr^{-1}) exceed FAO projections for N (Alexandratos and Bruinsma, 2012) for global fertilizer use in 2050 (140 Tg N yr^{-1} and 32 Tg P yr^{-1}) which underestimated the 2015 fertilizer use. The SSP scenarios form a range around these estimates as a result of the wide spectrum of assumptions on population growth, diets and agricultural efficiencies. The 2% decline for the SSP2 for N fertilizer use in the European Union (EU) for 2020–2030 is close to the 3% decline projected by Fertilizers Europe (Fertilizers Europe, 2019). For P, Fertilizers Europe projects an increase by 1%, while SSP2 points to a decline by 1%.

Previous work involved a very similar implementation of international scenarios, the Millennium Assessment (MA) scenarios (Bouwman et al., 2009). Fertilizer N projections were much lower than the current ones, primarily because the MA scenarios followed the agricultural efficiencies used in the FAO projection for 2015 and 2030 (Alexandratos, 1995; Bruinsma, 2003) which resulted in much lower estimates than the current ones. The actual 2015 N and P fertilizer use is already close to earlier scenario assessments for the year 2030 (Bouwman et al., 2005) based on FAO projections made around the year 2000 (Bruinsma, 2003), which illustrates the uncertainty in the projections of future crop production, technological change and fertilizer use efficiency. Our projections for agricultural N fixation exceed the MA estimates because a different method (Salvagiotti et al., 2008) was adopted, while for N fixation in natural ecosystems GNM uses much lower estimates based on recent insights (Vitousek et al., 2013).

Comparison of retention among models is difficult as nutrient removal depends on various factors such as the hydrology at the location of delivery to surface water, while the delivery of nutrients is often not specified by the models such as Global-NEWS (Seitzinger et al., 2010) and the Net Anthropogenic Nitrogen Inputs approach (NANI) (Boyer et al., 2006). River N export resulting from delivery and in-stream retention is uncertain, as illustrated by the wide range of estimates for the year 2000 from 40 Tg N yr^{-1} (Green et al., 2004) to 43 Tg N yr^{-1} according to Global NEWS and ~ 60 Tg N yr^{-1} by an earlier version of Global NEWS (Seitzinger et al., 2005) and the NANI approach (Boyer et al., 2006). A previous version of our model with a constant global export coefficient yielded estimates of 46–54 Tg N yr^{-1} (Bouwman et al., 2005; Van Drecht et al., 2003). Our global river N export for 2000 of 35 Tg N yr^{-1} is at the low end of the range of estimates. The global P export from IMAGE-GNM for 2000 (4 Tg P yr^{-1}) is much less than the Global NEWS estimate of (9 Tg P yr^{-1}) and the 22 Tg P yr^{-1} from Meybeck (1982). Global estimates for river P export exceeding 10 Tg P yr^{-1} seem unrealistic based on the validation of IMAGE-GNM (section 4.1).

4.3. Sources and pathways

The agricultural system is the major driver of the global nutrient cycles, as the N and P inputs in agricultural systems are by far the dominant inputs (Figs. 3 and 4). However, a large part of the N is removed in the harvested products, and surplus N is removed by denitrification, so that only a relatively small fraction finds its way to surface water or is stored temporarily in aquifers and sediments. Crop harvest is also an important sink for the P inputs in food production, and a large part of the surplus P is retained in soils where it is absorbed chemically and can contribute to future crop production. Only a minor fraction finds its way to surface water.

In the pathways by which nutrients are delivered to surface water there is a different pattern compared to the inputs. In 2015, N delivery to surface water from agriculture was important (globally 55% and close to 60% in industrialized countries), but natural sources (26%) and sewage (16%) also had a significant contribution. In most scenarios the agricultural contribution will increase somewhat in all world regions. The patterns for P are similar (58% from agriculture, 30% from natural sources and 12% from sewage).

The growing importance of sewage as a nutrient source in surface water is due to sanitation, improving drinking water supply and connection to public sewers, which is the most common sanitation option in urban areas. Agricultural sources are about half of the total river export, but sewage contributed one third at the global scale in 2015, and its share will increase further to 17 to 23% depending on the SSP considered. This phenomenon of an increasing share of nutrients from sewage during river transport occurs in all world regions, and is related to the development of large megacities in the coastal zone or in the middle and downstream parts of river basins in many countries. With shorter travel times, retention of this important nutrient input is declining.

The differences in retention between BRIC and ROW are related to the presence of water reservoirs and their impact on the water travel time in combination with water temperature, which in the tropical climates of many ROW countries exceeds that in temperate countries causing elevated retention rates. Finally, elevated N concentrations may negatively impact retention in polluted rivers by inhibiting denitrification (Mulholland et al., 2008).

Groundwater has a major impact on the N loading of surface waters. The contribution of groundwater stemming from agricultural areas contributed 32% to total N export in 1980 and 2015, and this contribution will increase to 37% of the total N export in the SSP3 scenario With the large amounts of N that are temporarily stored in groundwater, it is clear that this N legacy plays an important part in future scenarios (see Text S4). Surface runoff and erosion contribute around 18% to total river N export in all years. The absolute amount of P from surface runoff increased rapidly, but due to increasing delivery from sewage, its contribution as a fraction of total river export declined from 50 to 45% between 1980 and 2015, and will vary between 42 and 46 % in the scenarios for 2050.

4.4. Implications for SDG targets

Using the IMAGE implementations of the SSPs, a recent study (van Meijl et al., 2020) concluded that although globally malnutrition will decline in most SSPs, there will be a growing concentration of undernourishment in South Asia and Sub-Saharan Africa. Undernourishment is projected to continue to be high in SSP4 and to increase in SSP3, and the most rapid decline of undernourishment is achieved in SSP5 and less so in SSP1.

For SDG14 we assume that a reduction of nutrient loading implies a step towards achieving SDG14, while for SDG6 we take target 6.3 (71% of wastewater treated safely). Reductions of N and P delivery and export to coastal marine waters is achieved in SSP1 and SSP5 in industrialized and BRIC countries. Within the industrialized countries there are wide differences, with reductions in SSP1 and no or only small reductions in SSP3 in all IMAGE regions (Figure S3b-c), but similar reductions in SSP1 and SSP5 in USA, Western Europe and Japan but deviating changes in e.g. Canada and Oceania. Within BRIC, our results indicate an improvement in SSP1 and SSP5 in the Russian Federation and China, and no improvement in Brazil and India (Figure S3a). In ROW countries a reduction of nutrient pollution seems to be even more difficult (Figs. 3 and 4), with an improvement or stabilization in Mexico, Turkey, Middle East, and an increasing nutrient enrichment of inland waters and coastal seas in all developing countries in all scenarios (Figures S3d-h).

Recent work (Van Puijenbroek et al., 2019) using the same data presented in this paper showed that SDG6 target 6.3 will not be achieved in Sub-Saharan Africa and South Asia in any of the SSPs, primarily as a result of poverty, poorly functioning institutions and inequality (WHO/Unesco, 2017). Therefore, regions of the world where undernourishment will increasingly be concentrated are exactly those where SDG target 6.3 cannot be achieved and where nutrient enrichment is a threat to SDG 14.

Against the background of the increasing contribution of sewage to total nutrient loading in many parts of the world, our data suggest that the traditional sewage connection may not be the most logical option for simultaneously tackling health and water quality problems, especially considering the risk of depletion of economically accessible high quality P reserves for fertilizer production (Cordell et al., 2013; Cordell and White, 2014; Van Vuuren et al., 2010). Construction of sewage systems and wastewater treatment in large urban centers may technically be the easiest way to dispose of human waste and prevent diarrhea, even today a widespread problem and cause of 300,000 child deaths in 2016 (WHO, 2020). However, without effective water treatment there is a risk of, temporary, increase of N and P loads to river and coasts. As an alternative, sophisticated sewage systems with separate collection of urine from households could be a good option in future urban planning, in order to recycle the nutrients in farms or gardens. Our results show that this can substitute considerable amounts of N produced by Haber-Bosch and P from rock phosphate (Figs. 5-6 and S5-6). A further option for improved sanitation in combination with recycling of nutrients that may be most appropriate in rural areas is ecological sanitation (Langergraber and Muelleggera, 2005; Simha and Ganesapillai, 2017). This strategy is an example of combining policy ambitions for increased food security, resource efficiency and environmental quality in the SDGs, the GPA and the Colombo Declaration, which underlines the need for a coordination mechanism between UN conventions and resolutions (Sutton et al., 2019).

An important issue is the depletion of the world's phosphate reserves. The SSP projections of synthetic P fertilizer use in 2050 (31 Tg P yr^{-1} in SSP2, and 25 to 33 Tg P yr^{-1} in the other SSPs compared to the 21 Tg P yr^{-1} in 2015) imply rapidly increasing mining of rock phosphate. Since the worst case in SSP3 is close to the worst case in Van Vuuren et al. (2010), this would lead to around 60% depletion at the end of the 21st century.

Agriculture is the major anthropogenic nutrient source in most parts of the world. Hence, it is clear that reduction of emissions and increase of nutrient use efficiencies can lead to significant reductions of nutrient loading from agriculture. Considerable improvement of the efficiency of N use are assumed in the sustainability scenarios SSP1. The application of synthetic P fertilizers can be reduced considerably in countries where sufficient residual soil P reserves have been built up, such as in industrialized countries, China, India, the former Soviet Union. In many other countries, such as in Sub-Saharan Africa, soils have small P reserves, and chemically fix P. With this low P availability, application rates of P and N will have to increase considerably to achieve the yield projections in the various scenarios. This will almost inevitably lead to increasing nutrient losses to surface water. An essential element is soil conservation adapted to the local cropping system, climate, soil and terrain conditions to minimize P losses through erosion, and reduce soil carbon loss to secure the soil's long-term productivity, and the farm's future profitability (FAO, 2018). Our results indicate that nutrients that have been temporarily stored in the past, may lead to a legacy of past management which may interfere with policy strategies to reduce eutrophication of inland and coastal marine waters.

Finally, HAB risk in coastal waters may be increasing in environments where N is available in excess with respect to the "healthy" Redfield molar N:P ratio of 16 (Redfield et al., 1963), especially when N occurs in reduced forms (Glibert et al., 2014). Our results indicate that N:P ratios in river export to the coastal ocean show a decline in IND and BRIC and an increase in ROW countries in SSP1 (See Text S5 and Table S5). In all other SSPs, the N:P ratios in the river export will increase in BRIC and ROW and show a stabilization or a slight decline in IND countries. This results in increasing N:P ratios in rivers draining into the Indian Ocean in all scenarios except SSP1 (Fig. 8).

5. Conclusions

Natural sources of nutrients have been declining in the past and will continue to decline in all scenarios due to massive land transformations, while anthropogenic sources (agriculture, sewage, aquaculture) are increasing and thus becoming increasingly dominant in 2050 (globally up to 80% of nutrient delivery).

In SSP2-5, inputs, delivery and export of N and P show major increases. Slowing-down of nutrient cycles is hard to achieve, since even in the more environmentally friendly SSP1 scenario the slower increase in agricultural production, the higher efficiency and the improvements in sanitation, do not lead to a reduction of total N and P river export. To reduce global N and P export, more efforts are needed than those employed in SSP1, such as further reductions in consumption of animal products, better integration of crop and livestock production systems to close nutrient cycles, technological change towards agricultural nutrient use efficiencies close to those obtained in experimental fields, and advanced wastewater treatment to replace primary and secondary installations. This poses another challenge in the achievement of SGD2 (zero hunger).

Point sources are an important and increasing source of freshwater and marine pollution, due to increasing urban populations with connection to sewage systems. In view of its growing water pollution and P depletion as a threat to future fertilizer production, sewage connection may not be the most logical option for tackling both health and water quality problems. Systems that can deal with health issues and at the same time help to capture the large N and P flows in human waste are needed. Completely different approaches for solving sanitation problems than currently envisaged are therefore needed to help achieving SDG6 (clean water and sanitation).

The enormous amounts of N that are temporarily stored in groundwater and P accumulation in sediments may in future release dissolved reactive N and P that are not controllable by environmental management and form unwanted and unexpected sources of nutrients.

The tendency towards increasing N:P ratios in fertilizers, wastewater treatment systems that are more efficient for P than for N, and of river basins with more efficient P than N retention, and possibly contributions from groundwater legacies is causing elevated and increasing N:P ratios in the water draining into the world's coastal ocean. This has been shown to be one of the drivers of the increasing proliferation of harmful algal blooms. The scenario which has the strongest ambition to protect the environment, SSP1, is leading to even higher N:P ratios than the other scenarios in large parts of the world.

Integrated global assessments that consistently address the linkages between N and P in all economic and biophysical systems on the land–water-air continuum, as presented here, are vital to address the nutrient nexus towards a greener economy that delivers food and energy security with less environmental pollution. This double ambition is a key topic for the UN Food Systems summit in New York in 2021. This study highlights that combined achievement of SDG2 (zero hunger), SDG6 (clean water and sanitation) and SDG14 (life below water) is possible with decreasing global inputs of new N and P. This not only requires a reduction of food loss and waste, and of meat and dairy consumption in developed countries (Westhoek et al., 2021; Westhoek et al., 2016) but also a more balanced local and regional management and global redistribution of inputs for both N and P that accounts for future nutrient legacies.

Declaration of Competing Interest

The authors declare that they have no known competing financial interests or personal relationships that could have appeared to influence the work reported in this paper.

Acknowledgements

PBL received funding for this work from the International Nitrogen Management System project (INMS, http://www.inms.international/) funded by GEF and implemented by UNEP. A.F. Bouwman and A.H.W. Beusen received support from PBL Netherlands Environmental Assessment Agency through in-kind contributions to The New Delta 2014 ALW project no. 869.15.015 and no. 869.15.014.

Appendix A. Supplementary data

Supplementary data to this article can be found online at https://doi.org/10.1016/j.gloenvcha.2021.102426.

References

Alexandratos, N., 1995. World agriculture: towards 2010. Wiley and Sons, Chichester.
Alexandratos, N., Bruinsma, J., (2012) World Agriculture Towards 2030/2050. The 2012 revision. Food and Agriculture Organization of the United Nations, Rome.
Beusen, A., Bouwman, A., Van Beek, L.P.H., Mogollon, J., Middelburg, J.J. (2016) Global riverine N and P transport to ocean increased during the 20th century despite increased retention along the aquatic continuum. Biogeosciences 13, 2441-2451, https//doi.org/10.5194/bg-13-2441-2016.
Beusen, A.H.W., Bouwman, A.F., Heuberger, P.S.C., Van Drecht, G., Van Der Hoek, K.W., 2008. Bottom-up uncertainty estimates of global ammonia emissions from global agricultural production systems. Atmos. Environ. 42 (24), 6067–6077.
Beusen, A.H.W., Van Beek, L.P.H., Bouwman, A.F., Mogollón, J.M., Middelburg, J.J., 2015. Coupling global models for hydrology and nutrient loading to simulate nitrogen and phosphorus retention in surface water. Description of IMAGE-GNM and analysis of performance. Geosci. Model Dev. 8 (12), 4045–4067.
Bondeau, A., Smith, P.C., Zaehle, S., Nke, Schaphoff, S., Lucht, W., Cramer, W., Gerten, D., Lotze-Campen, H., Ller, C., Reichstein, M., Smith, B., 2007. Modelling the role of agriculture for the 20th century global terrestrial carbon balance. Glob. Change Biol. 13 (3), 679–706.
Bouwman, A.F., Beusen, A.H.W., Lassaletta, L., Van Apeldoorn, D.F., Van Grinsven, H.J. M., Zhang, J., Van Ittersum, M.K., 2017. Lessons from temporal and spatial patterns in global use of N and P fertilizer on cropland. Sci. Rep. 7 (1) https://doi.org/10.1038/srep40366.
Bouwman, A.F., Beusen, A.H.W., Billen, G., 2009. Human alteration of the global nitrogen and phosphorus soil balances for the period 1970-2050: Nitrogen and phosphorus balances. Global Biogeochem. Cycles 23 (4). https://doi.org/10.1029/2009GB003576.
Bouwman, A.F., Beusen, A.H.W., Griffioen, J., Van Groenigen, J.W., Hefting, M.M., Oenema, O., Van Puijenbroek, P.J.T.M., Seitzinger, S., Slomp, C.P., Stehfest, E., 2013a. Global trends and uncertainties in terrestrial denitrification and N2O

emissions. Phil. Trans. R. Soc. B 368 (1621), 20130112. https://doi.org/10.1098/rstb.2013.0112.
Bouwman, A.F., Boumans, L.J.M., Batjes, N.H., 2002. Estimation of global NH3 volatilization loss from synthetic fertilizers and animal manure applied to arable lands and grasslands. Global Biogeochem. Cycles 16, 1024. https://doi.org/10.1029/2000GB001389.
Bouwman, L., Goldewijk, K.K., Van Der Hoek, K.W., Beusen, A.H.W., Van Vuuren, D.P., Willems, J., Rufino, M.C., Stehfest, E., 2013b. Exploring global changes in nitrogen and phosphorus cycles in agriculture induced by livestock production over the 1900-2050 period. Proc. Natl. Acad. Sci. 110 (52), 20882–20887.
Bouwman, A.F., Van Drecht, G., Knoop, J.M., Beusen, A.H.W., Meinardi, C.R., 2005. Exploring changes in river nitrogen export the the world's oceans. Global Biogeochem. Cycles 19, GB1002. https://doi.org/10.1029/2004GB002314.
Boyer, E.W., Howarth, R.W., Galloway, J.N., Dentener, F.J., Green, P.A., Vörösmarty, C. J., 2006. Riverine nitrogen export from the continents to the coasts. Global Biogeochem. Cycles 20 (1), n/a–n/a.
Bruinsma, J.E., 2003. World agriculture: towards 2015/2030. An FAO perspective, Earthscan, London.
Cordell, D., Jackson, M., White, S., 2013. Phosphorus flows through the Australian food system: Identifying intervention points as a roadmap to phosphorus security. Environ. Sci. Policy 29, 87–102.
Cordell, D., White, S., 2014. Life's Bottleneck: Sustaining the World's Phosphorus for a Food Secure Future. Annu. Rev. Environ. Resour. 39 (1), 161–188.
Diaz, R.J., Rosenberg, R., 2008. Spreading dead zones and consequences for marine ecosystems. Science 321 (5891), 926–929.
Doelman, J.C., Stehfest, E., Tabeau, A., Van Meijl, H., Lassaletta, L., Gernaat, D.E.H.J., Hermans, K., Harmsen, M., Daioglou, V., Biemans, H., Van Der Sluis, S., Van Vuuren, D.P., 2018. Exploring SSP land-use dynamics using the IMAGE model: Regional and gridded scenarios of land-use change and land-based climate change mitigation. Global Environ. Change 48, 119–135.
FAO, (2018) The future of food and agriculture – Alternative pathways to 2050. Food and Agriculture Organization of the United Nations, Rome, 224 pp. Licence:CC BY-NC-SA 3.0 IGO.
FAO, (2020) FishStatJ - Software for Fishery and Aquaculture Statistical Time Series. http://www.fao.org/fishery/statistics/software/fishstatj/en. Fisheries and Aquaculture Information and Statistics Service, Food and Agriculture Organization of the United Nations, retrieved 30 October 2020, Rome.
Fertilizers Europe, (2019) Forecast of food, farming and fertilizer use in the European Union 2019-2029. European Fertilizer Manufacturers Association, Brussels, p. 20.
Forsberg, B.R., Devol, A.H., Richey, J.E., Martinelli, L.A., Dos Santos, H., 1988. Factors controlling nutrient concentrations in Amazon floodplain lakes. Limnol. Oceanogr. 33, 41–56.
Fowler, D., Coyle, M., Skiba, U., Sutton, M.A., Cape, J.N., Reis, S., Sheppard, L.J., Jenkins, A., Grizzetti, B., Galloway, J.N., Vitousek, P., Leach, A., Bouwman, A.F., Butterbach-Bahl, K., Dentener, F., Stevenson, D., Amann, M., Voss, M. (2013) The global nitrogen cycle in the twenty-first century. Philosophical Transactions of the Royal Society B: Biological Sciences 368, https//doi.org/ 10.1098/rstb.2013.0164.
Galloway, J.N., Cowling, E.B., 2002. Reactive nitrogen and the world: 200 years of change. Ambio 31 (2), 64–71.
Galloway, J.N., Dentener, F.J., Capone, D.G., Boyer, E.W., Howarth, R.W., Seitzinger, S. P., Asner, G.P., Cleveland, C.C., Green, P.A., Holland, E.A., Karl, D.M., Michaels, A. F., Porter, J.H., Townsend, A.R., Vörösmarty, C.J., 2004. Nitrogen Cycles: Past, Present, and Future. Biogeochemistry 70 (2), 153–226.
Galloway, J.N., Schlesinger, W.H., Levy, H., Michaels, A., Schnoor, J.L., 1995. Nitrogen fixation: anthropogenic enhancement-environmental response. Global Biogeochem. Cycles 9 (2), 235–252.
Giller, K.E., Chalk, P., Dobermann, A., Hammond, L., Heffer, P., Ladha, J.K., Nyamudeza, P., Maene, L., Ssali, H., Freney, J., 2004. Emerging technologies to increase the efficiency of use of fertilizer nitrogen. In: Mosier, A.R., Syers, J.K., Freney, J.R. (Eds.), Agriculture and the nitrogen cycle. Island Press, Washington, D. C., pp. 35–51
Glibert, P.M., Maranger, R., Sobota, D.J., Bouwman, L., 2014. The Haber Bosch-harmful algal bloom (HB-HAB) link. Environ. Res. Lett. 9 (10), 105001. https://doi.org/10.1088/1748-9326/9/10/105001.
Green, P.A., Vörösmarty, C.J., Meybeck, M., Galloway, J.N., Peterson, B.J., Boyer, E.W., 2004. Pre-industrial and contemporary fluxes of nitrogen through rivers: a global assessment based on typology. Biogeochemistry 68 (1), 71–105.
Harris, I., Jones, P.D., Osborn, T.J., Lister, D.H., 2014. Updated high-resolution grids of monthly climatic observations – the CRU TS3.10 Dataset. International Journal of Climatology 34, 623–642. https://doi.org/10.1002/joc.3711.
Hempel, S., Frieler, K., Warszawski, L., Schewe, J., Piontek, F., 2013. A trend-preserving bias correction – the ISI-MIP approach. Earth Syst. Dynam. 4, 219–236. https://doi.org/10.5194/esd-4-219-2013.
Howarth, R., Chan, F., Conley, D.J., Garnier, J., Doney, S.C., Marino, R., Billen, G., 2011. Coupled biogeochemical cycles: eutrophication and hypoxia in temperate estuaries and coastal marine ecosystems. Front. Ecol. Environ. 9 (1), 18–26.
Klein Goldewijk, K., Beusen, A., Janssen, P., 2010. Long-term dynamic modeling of global population and built-up area in a spatially explicit way: HYDE 3.1. Holocene 20 (4), 565–573.
Langergraber, G., Muellegger, E., 2005. Ecological Sanitation—a way to solve global sanitation problems? Environ. Int. 31 (3), 433–444.
Lassaletta, L., Billen, G., Grizzetti, B., Anglade, J., Garnier, J., 2014. 50 year trends in nitrogen use efficiency of world cropping systems: The relationship between yield and nitrogen input to cropland. Environ. Res. Lett. 9 (10), 105011. https://doi.org/10.1088/1748-9326/9/10/105011.
Li, S., Bush, R.T., 2015. Changing fluxes of carbon and other solutes from the Mekong River. Sci Rep 5 (1). https://doi.org/10.1038/srep16005.
MetOffice (2020) HadCM3: Met Office climate prediction model. https://www.metoffice.gov.uk/research/approach/modelling-systems/unified-model/climate-models/hadcm3.
Meybeck, M., 1982. Carbon, nitrogen and phosphorous transport by world rivers. Am. J. Sci. 282, 401–450.
Michalak, A.M., Anderson, E.J., Beletsky, D., Boland, S., Bosch, N.S., Bridgeman, T.B., Chaffin, J.D., Cho, K., Confesor, R., Daloglu, I., DePinto, J.V., Evans, M.A., Fahnenstiel, G.L., He, L., Ho, J.C., Jenkins, L., Johengen, T.H., Kuo, K.C., LaPorte, E., Liu, X., McWilliams, M.R., Moore, M.R., Posselt, D.J., Richards, R.P., Scavia, D., Steiner, A.L., Verhamme, E., Wright, D.M., Zagorski, M.A., 2013. Record-setting algal bloom in Lake Erie caused by agricultural and meteorological trends consistent with expected future conditions. Proc. Natl. Acad. Sci. 110 (16), 6448–6452.
Mogollón, J.M., Beusen, A.H.W., Van Grinsven, H.J.M., Westhoek, H., Bouwman, A.F., 2018. Future agricultural phosphorus demand according to the shared socio-economic pathways. Global Environmental Change 50, 149–163. https://doi.org/10.1016/j.gloenvcha.2018.03.007.
Mooij, W.M., Van Wijk, D., Beusen, A.H.W., Brederveld, R.J., Chang, M., Cobben, M.M. P., DeAngelis, D.L., Downing, A.S., Green, P., Gsell, A.S., Huttunen, I., Janse, J.H., Janssen, A.B.G., Hengeveld, G.M., Kong, X., Kramer, L., Kuiper, J.J., Langan, S.J., Nolet, B.A., Nuijten, R.J.M., Strokal, M., Troost, T.A., Van Dam, A.A., Teurlincx, S., 2019. Modeling water quality in the Anthropocene: directions for the next-generation aquatic ecosystem models. Curr. Opin. Environ. Sustain. 36, 85–95. https://doi.org/10.1016/j.cosust.2018.10.012.
Morée, A.L., Beusen, A.H.W., Bouwman, A.F., Willems, W.J., 2013. Exploring global nitrogen and phosphorus flows in urban wastes during the twentieth century: twentieth century urban N and P flows. Global Biogeochem. Cycles 27 (3), 836–846.
Mulholland, P.J., Helton, A.M., Poole, G.C., Hall, R.O., Hamilton, S.K., Peterson, B.J., Tank, J.L., Ashkenas, L.R., Cooper, L.W., Dahm, C.N., Dodds, W.K., Findlay, S.E.G., Gregory, S.V., Grimm, N.B., Johnson, S.L., McDowell, W.H., Meyer, J.L., Valett, H. M., Webster, J.R., Arango, C.P., Beaulieu, J.J., Bernot, M.J., Burgin, A.J., Crenshaw, C.L., Johnson, L.T., Niederlehner, B.R., O'Brien, J.M., Potter, J.D., Sheibley, R.W., Sobota, D.J., Thomas, S.M., 2008. Stream denitrification across biomes and its response to anthropogenic nitrate loading. Nature 452 (7184), 202–205.
Newbold, J.D., Elwood, J.W., O'Neill, R.V., Winkle, W.V., 1981. Measuring nutrient spiraling in streams. Can. J. Fish. Aquat. Sci. 38, 860–863.
O'Neill, B.C., Kriegler, E., Riahi, K., Ebi, K.L., Hallegatte, S., Carter, T.R., Mathur, R., Van Vuuren, D.P., 2014. A new scenario framework for climate change research: the concept of shared socioeconomic pathways. Clim. Change 122 (3), 387–400.
Poli, P., Hersbach, H., Dee, D.P., Berrisford, P., Simmons, A.J., Vitart, F., Laloyaux, P., Tan, D.G.H., Peubey, C., Thépaut, J.-N., Trémolet, Y., Hólm, E.V., Bonavita, M., Isaksen, L., Fisher, M., 2016. ERA-20C: an atmospheric reanalysis of the twentieth century. J. Clim. 29 (11), 4083–4097.
Rabalais, N.N., Turner, R.E., Wiseman, W.J., 2001. Hypoxia in the Gulf of Mexico. J. Environ. Qual. 30 (2), 320–329.
Redfield, A.C., Ketchum, B.H., Richards, F.A., 1963. The influence of organisms on the composition of sea-water. In: Hills, M.N. (Ed.), The sea. Wiley and Sons, New York, pp. 12–37.
Riahi, K., Van Vuuren, D.P., Kriegler, E., Edmonds, J., O'Neill, B.C., Fujimori, S., Bauer, N., Calvin, K., Dellink, R., Fricko, O., Lutz, W., Popp, A., Cuaresma, J.C., Kc, S., Leimbach, M., Jiang, L., Kram, T., Rao, S., Emmerling, J., Ebi, K., Hasegawa, T., Havlik, P., Humpenöder, F., Da Silva, L.A., Smith, S., Stehfest, E., Bosetti, V., Eom, J., Gernaat, D., Masui, T., Rogelj, J., Strefler, J., Drouet, L., Krey, V., Luderer, G., Harmsen, M., Takahashi, K., Baumstark, L., Doelman, J.C., Kainuma, M., Klimont, Z., Marangoni, G., Lotze-Campen, H., Obersteiner, M., Tabeau, A., Tavoni, M., 2017. The Shared Socioeconomic Pathways and their energy, land use, and greenhouse gas emissions implications: An overview. Global Environ. Change 42, 153–168. https://doi.org/10.1016/j.gloenvcha.2016.05.009.
Ritchie, H., (2018) Urbanization. Published online at OurWorldInData.org. Retrieved from: 'https://ourworldindata.org/urbanization'.
Salvagiotti, F., Cassman, K.G., Specht, J.E., Walters, D.T., Weiss, A., Dobermann, A., 2008. Nitrogen uptake, fixation and response to fertilizer N in soybeans: A review. Field Crops Research 108 (1), 1–13.
Sattari, S.Z., Bouwman, A.F., Martinez Rodríguez, R., Beusen, A.H.W., Van Ittersum, M. K., 2016. Negative global phosphorus budgets challenge sustainable intensification of grasslands. Nat Commun 7 (1). https://doi.org/10.1038/ncomms10696.
Seitzinger, S.P., Harrison, J.A., Dumont, E., Beusen, A.H.W., Bouwman, A.F., 2005. Sources and delivery of carbon, nitrogen, and phosphorus to the coastal zone: An overview of Global Nutrient Export from Watersheds (NEWS) models and their application. Global Biogeochem. Cycles 19 (4). https://doi.org/10.1029/2005GB002606.
Seitzinger, S.P., Mayorga, E., Bouwman, A.F., Kroeze, C., Beusen, A.H.W., Billen, G., Van Drecht, G., Dumont, E., Fekete, B.M., Garnier, J., Harrison, J.A., 2010. Global river nutrient export: A scenario analysis of past and future trends. Global Biogeochem. Cycles 24 (4). https://doi.org/10.1029/2009GB003576.
Simha, P., Ganesapillai, M., 2017. Ecological Sanitation and nutrient recovery from human urine: How far have we come? A review. Sustainable Environ. Res. 27, 107–116. https://doi.org/10.1016/j.serj.2016.12.001.
Smil, V. (2000) Phosphorus in the environment: natural flows and human interferences. Annual Review of Energy and the Environment 25, 53-88, https//doi.org/ 10.1146/annurev.energy.25.1.53.
Smil, V., 2001. Enriching the earth: Fritz Haber, Carl Bosch, and the transformation of world food. MIT Press, Cambridge.

Stehfest, E., Van Vuuren, D.P., Kram, T., Bouwman, A.F. (2014) Integrated Assessment of Global Environmental Change with IMAGE 3.0. Model description and policy applications. PBL Netherlands Environmental Assessment Agency (http://themasites.pbl.nl/models/image/index.php/Main_Page), The Hague.
Strahler, A.N., 1957. Quantitative analysis of watershed geomorphology. Transactions of the American Geophysical Union 38 (6), 913. https://doi.org/10.1029/TR038i006p00913.
Workshop, S.S., 1990. Concepts and methods for assessing solute dynamics in stream ecosystems. Journal of the North American Benthological Society 9 (2), 95–119.
Sutanudjaja, E.H., Van Beek, R., Wanders, N., Wada, Y., Bosmans, J.H.C., Drost, N., Van Der Ent, R.J., De Graaf, I.E.M., Hoch, J.M., De Jong, K., Karssenberg, D., López López, P., Peßenteiner, S., Schmitz, O., Straatsma, M.W., Vannametee, E., Wisser, D., Bierkens, M.F.P. (2018) PCR-GLOBWB 2: A 5 arcmin global hydrological and water resources model. Geoscientific Model Development 11, 2429-2453, https//doi.org/10.5194/gmd-11-2429-2018.
Sutton, M., Raghuram, N., Adhya, T.K., Baron, J., Cox, C., De Vries, W., Hicks, K., Howard, C., Ju, X., Kanter, D., Masso, C., Ometto, J.-P., Ramachandran, R., Van Grinsven, H., Winiwarter, W., 2019. The nitrogen fix: from nitrogen cycle pollution to nitrogen circular economy. UN Environment, Nairobi.
Turner, R.E., Rabalais, N.N., Justic, D., Dortch, Q., 2003. Global patterns of dissolved N, P and Si in large rivers. Biogeochemistry 64, 297–317.
UN, (2020) World population prospects: the 2019 revision. United Nations Department for Economic and Social Affairs (https://population.un.org/wpp/) accessed 14 August 2020, New York.
UN Environment, (2019a) Colombo Declaration (https://www.unep.org/news-and-stories/press-release/colombo-declaration-calls-tackling-global-nitrogen-challenge), UN Environment, Nairobi.
UN Environment (2019b) Global Environment Outlook – GEO-6: Summary for Policymakers. Cambridge University Press, Cambridge.
UNEP, (2019) Resolution adopted by the United Nations Environment Assembly on 15 March 2019. UNEP/EA.4/Res.14, United Nations Environment Programme, Nairobi.
United Nations, (1995) Global Programme of Action for the Protection of the Marine Environment from Land-Based Activities (https://www.un.org/press/en/1995/19951108.he915.html).
Van Beek, L.P.H., Wada, Y., Bierkens, M.F.P. (2011) Global monthly water stress: 1. Water balance and water availability. Water Resour. Res. 47, W07517, https//doi.org/ 10.1029/2010wr009791.
Van Dijk, K.C., Lesschen, J.P., Oenema, O., 2016. Phosphorus flows and balances of the European Union Member States. Sci. Total Environ. 542, 1078–1093. https://doi.org/10.1016/j.scitotenv.2015.08.048.
Van Drecht, G., Bouwman, A.F., Knoop, J.M., Beusen, A.H.W., Meinardi, C.R., 2003. Global modeling of the fate of nitrogen from point and nonpoint sources in soils, groundwater and surface water. Global Biogeochem. Cycles 17 (4), n/a–n/a. https://doi.org/10.1029/2003GB002060.
Van Meijl, H., Tabeau, A., Stehfest, E., Doelman, J., Lucas, P., 2020. How food secure are the green, rocky and middle roads: food security effects in different world development paths. Environ. Res. Commun. 2 (3), 031002. https://doi.org/10.1088/2515-7620/ab7aba.
Van Puijenbroek, P.J.T.M., Beusen, A.H.W., Bouwman, A.F., 2019. Global nitrogen and phosphorus in urban waste water based on the Shared Socio-economic pathways. J. Environ. Manage. 231, 446–456.
Van Vuuren, D.P., Bouwman, A.F., Beusen, A.H.W., 2010. Phosphorus demand for the 1970–2100 period: a scenario analysis of resource depletion. Global Environ. Change 20 (3), 428–439.
Van Vuuren, D.P., Kriegler, E., O'Neill, B.C., Ebi, K.L., Riahi, K., Carter, T.R., Edmonds, J., Hallegatte, S., Kram, T., Mathur, R., Winkler, H., 2014. A new scenario framework for Climate Change Research: scenario matrix architecture. Clim. Change 122 (3), 373–386.
Van Vuuren, D.P., Stehfest, E., Gernaat, D.E.H.J., Doelman, J.C., Van Den Berg, M., Harmsen, M., De Boer, H.S., Bouwman, L.F., Daioglou, V., Edelenbosch, O.Y., Girod, B., Kram, T., Lassaletta, L., Lucas, P.L., Van Meijl, H., Müller, C., Van Ruijven, B.J., Van der Sluis, S., Tabeau, A., 2017. Energy, land-use and greenhouse gas emissions trajectories under a green growth paradigm. Global Environ. Change 42, 237–250.
Vitousek, P.M., Menge, D.N.L., Reed, S.C., Cleveland, C.C., 2013. Biological nitrogen fixation: rates, patterns and ecological controls in terrestrial ecosystems. Phil. Trans. R. Soc. B 368 (1621), 20130119. https://doi.org/10.1098/rstb.2013.0119.
Vollenweider, R.A., 1992. Coastal marine eutrophication: principles and control. Science of The Total Environment Supplement 1992, 1–20.
Westhoek, H., Doelman, J.C., Muilwijk, H., Stehfest, E., 2021. Commentary: Food choices and environmental impacts: Achievements and challenges. Global Environ. Change 102402. https://doi.org/10.1016/j.gloenvcha.2021.102402.
Westhoek, H., Ingram, J., Van Berkum, S., Özay, L., Hajer, M., (2016) Food Systems and Natural Resources. A Report of the Working Group on Food Systems of the International Resource Panel. United Nations Environment Programme, Nairobi (https://www.resourcepanel.org/sites/default/files/documents/document/media/food_systems_summary_report_english.pdf).
WHO, (2020) World Health Statistics 2020. Monitoring health for the SDGs sustainable development goals. World Health Organization. Licence: CC BY-NC-SA 3.0 IGO, Geneva.
WHO/Unesco, (2017) Progress on drinking water, sanitation and hygiene: 2017 update and SDG baselines, World Health Organization, Geneva.
Wollheim, W.M., Vörösmarty, C.J., Bouwman, A.F., Green, P., Harrison, J., Linder, E., Peterson, B.J., Seitzinger, S.P., Syvitski, J.P.M., 2008. Global N removal by freshwater aquatic systems using a spatially distributed, within-basin approach. Global Biogeochem. Cycles 22 (2). https://doi.org/10.1029/2007GB002963.
Woltjer, G.B., Kuiper, M.H., (2014) The MAGNET Model: Module description. LEI Wageningen UR (University & Research centre), Wageningen, p. 146.
Zhang, J., Beusen, A.H.W., Van Apeldoorn, D.F., Mogollón, J.M., Yu, C., Bouwman, A.F. (2017) Spatiotemporal dynamics of soil phosphorus and crop uptake in global cropland during the 20th century. Biogeosciences 14, 2055-2068, https//doi.org/10.5194/bg-14-2055-2017.
Zhang, X., Davidson, E.A., Mauzerall, D.L., Searchinger, T.D., Dumas, P., Shen, Y., 2015. Managing nitrogen for sustainable development. Nature 528 (7580), 51–59.
Zhang, X., Fang, Q., Zhang, T., Ma, W., Velthof, G.L., Hou, Y., Oenema, O., Zhang, F., 2020. Benefits and trade-offs of replacing synthetic fertilizers by animal manures in crop production in China: A meta-analysis. Glob. Change Biol. 26, 888–900. https://doi.org/10.1111/gcb.14826.